Final Technical Report on SBIR Project DE-FG02-04ER84016

Overview and Summary

Ionization Cooling using Parametric Resonances was an SBIR project begun in July 2004 and ended in January 2008 with Muons, Inc., (Dr. Rolland Johnson, PI), and Thomas Jefferson National Accelerator Facility (JLab) (Dr. Yaroslav Derbenev, Subcontract PI). The project was to develop the theory and simulations of Parametric-resonance Ionization Cooling (PIC) so that it could be used to provide the extra transverse cooling needed for muon colliders in order to relax the requirements on the proton driver, reduce the site boundary radiation, and provide a better environment for experiments.

During the course of the project, the theoretical understanding of PIC was developed [1,2] and a final exposition is ready for publication [Appendix I]. Workshops were sponsored by Muons, Inc. in May and September of 2007 that were devoted to the PIC technique [3]. One outcome of the workshops was the interesting and somewhat unexpected realization that the beam emittances using the PIC technique can get small enough that space charge forces can be important. A parallel effort to develop our G4beamline simulation program to include space charge effects was initiated to address this problem [4]. A method of compensating for chromatic aberrations by employing synchrotron motion was developed and simulated [5 and Appendix II]. A method of compensating for spherical aberrations using beamline symmetry was also developed and simulated [6 and Appendix III]. Different optics designs have been developed [7] using the OptiM program in preparation for applying our G4beamline simulation program, which contains all the power of the Geant4 toolkit.

However, no PIC channel design that has been developed has had the desired cooling performance when subjected to the complete G4beamline simulation program. This is believed to be the consequence of the difficulties of correcting the aberrations associated with the naturally large beam angles and beam sizes of the PIC method that are exacerbated by the fringe fields of the rather complicated channel designs that have been attempted. That is, while the designs developed and tested using the matrix program OptiM can work well, a real simulation with lumped dipoles, quadrupoles, and solenoids and their associated fringe fields has not succeeded. As a consequence of this realization, a new approach is being attempted that is based on the use of a helical solenoid (HS) channel that is made of simple coils that provide a much more homogeneous magnetic field. However, in order to use the HS a new approach was required to generate a variable dispersion that is needed according to the PIC theory described above. This approach and its first implementation will be described at EPAC08 in June, 2008 [8].

In the sections of the report that follow, the general theory of muon beam cooling is described starting from the basic ideas of ionization cooling and ending with the PIC ideas that have been developed in this project. The detailed theory of PIC is presented in Appendix I. The most important papers of the project are presented in subsequent appendices.

Final Technical Report on SBIR Project DE-FG02-04ER84016

Ionization Cooling using Parametric Resonances
by
Muons, Inc. and Thomas Jefferson National Accelerator Laboratory

Table of Contents

1. DOE award number: STTR Project DE-FG02-04ER84016,
Name of Recipient: Muons, Inc.

2. Project Title: Ionization Cooling using Parametric Resonances
Name of PI: Dr. Rolland P. Johnson
Research Partner: Thomas Jefferson National Accelerator Facility
Name of JLab subgrant PI: Dr. Yaroslav Derbenev

3. Date of Report: June 6, 2008
Period of Report: July, 2004 to June, 2008

4. Comparison of accomplishments and Goals:
The Goals and Milestones taken from the Phase II proposal are shown in italics and are followed by comments on accomplishments.

What was planned for the Phase II project.
Phase II plans are to develop the theory and simulations to the point that transverse cooling using parametric resonances is accepted as a way to relax the requirements on the proton driver, reduce the site boundary radiation, and provide a better environment for experiments at muon colliders. This will require additional theoretical development of techniques for control of aberrations and other higher order effects and for simultaneous emittance exchange to maintain small momentum spread. Complete simulations using realistic models of all components of the parametric resonance cooling channel will also be required.

.***Phase II Performance Schedule (Tasks and Milestones)***
PRSTAB paper covering PIC theory submitted
G4Beamline simulations demonstrate the general features of the theory
Space charge detuning relevance determined, effect mitigated if needed to be
G4Beamline models include all detuning compensation schemes
Emittance exchange based on PIC wedge absorbers modeled
Systematic investigation of PIC with compensations done for candidate lines, rings
Longitudinal PIC theory developed, evaluated for applications
Complete PIC scheme simulated as part of complete muon cooling line for a collider

5. Discussion of Accomplishments:

A preprint of the PRSTAB paper covering PIC theory is shown as Appendix I below. The aberration correction discussion is much more complete than we thought possible.

G4Beamline simulations have demonstrated the general features of the theory but they have not succeeded to demonstrate a useful example of a buildable beam line. The problem turned out to be much harder than we anticipated. However after many months of trying several alternative approaches, we believe that we have a good candidate beam line that is based on a helical solenoid design. First results will be presented at EPAC08.

Space charge detuning was found to be important for the final PIC cooling stages. This generated two relevant parallel developments. First, our G4Beamline program has been funded for upgrades that include space charge effects. Second, the use of muon bunch coalescing, a procedure proposed in a companion STTR project, allows the effect to be mitigated by reducing

the charge per bunch in the PIC stage of cooling. That is, several lower intensity muon bunches can be cooled by PIC at low energy, accelerated to an energy where space charge is not a problem, and then collected into a single RF bunch for use in a collider.

Although G4Beamline models were studied with realistic magnetic fields, the most useful program for studying the chromatic, spherical, and symmetry-dependent aberrations turned out to be OptiM. These studies are shown in Appendices II and III.

The theory of emittance exchange based on PIC wedge absorbers is included in Appendix I. The incorporation of a realistic wedge absorber scheme with G4beamline simulations must await the development of the HS model described below, as will systematic investigations of compensation techniques needed for a complete cooling line for a muon collider.

So far, no realistic use for longitudinal PIC has yet been considered.

6. Project Cost Status (Phase I plus Phase II):

As of June 6, 2008

	Spent	Budget	Remaining
JLab	89,811	90,000	189
Muons, Inc.	656,335	655,193	(953)
Total	746,146	745,193	(764)

7. Schedule Status:
The funds covered by the SBIR grant have been expended but the ultimate goal of the project to have a design for a fully simulated PIC channel is only partially completed.

8. Changes in Approach:
As discussed in the next section, a different solution to the beam line design has been proposed based on a helical solenoid magnet system. This may allow the full simulation to demonstrate the power of the PIC technique.

9. Actual or Anticipated Problems or Delays:
The original schedule for the Phase II project called for the hiring of a post doctoral research assistant at JLab to work on the simulations of the PIC process using the G4beamline program. Unfortunately, a hiring freeze at JLab prevented the advertizing and hiring for the position even though the position would be covered entirely by this grant. After a delay of four months, it was agreed that Muons, Inc. would recruit and hire a person for this task. Dr.David Newsham was hired in November 2005 to fulfill this role.

The analytical efforts of the project were successful in that the complete theory was developed and the space charge limitations were mitigated by the muon bunch coalescing technique. The effort to use the full G4beamline program to simulate a PIC channel was largely carried out by Dr. Newsham under the guidance of Dr. Derbenev and Dr. Bogacz of JLab. Several conference reports documented the efforts. A no-cost extension was granted to continue the search for a solution to the beamline design that would be compatible with the aberration control magnets.

Literally at the last days of the project, it was suggested that a beam line made of helical solenoid magnets would have the necessary field homogeneity to allow the PIC process to work. Some success on this project will be reported at EPAC08.

10. Changes or Absence of Key Personnel or Arrangements:
None except as noted in the previous section.

11. Products or Technology Transfer:

a. Publications and Conference Papers:

A paper to be submitted for publication and three conference papers are included in this document as four appendices. The abstract below describes a conference contribution that was supported in part by this grant.

Low Emittance Muon Colliders

Rolland Johnson for the Muons, Inc. Collaboration

Advances in ionization cooling, phase space manipulations, and technologies to achieve high brightness muon beams are stimulating designs of high-luminosity energy-frontier muon colliders. Simulations of Helical Cooling Channels (HCC) show impressive emittance reductions, new ideas on reverse emittance exchange and muon bunch coalescing are being developed, and high-field superconductors show great promise to improve the effectiveness of ionization cooling. Experiments to study RF cavities pressurized with hydrogen gas in strong magnetic fields have had encouraging results. A 6-dimensional HCC demonstration experiment is being designed and a 1.5 TeV muon collider is being studied at Fermilab. Two new synergies are that very cool muon beams can be accelerated in ILC RF structures and that this capability can be used both for muon colliders and for neutrino factories. These advances are discussed in the context of muon colliders with small transverse emittances and with fewer muons to ease requirements on site boundary radiation, detector backgrounds, and muon production.

The work described here was supported in part by DOE SBIR/STTR grants DE-FG02-03ER83722, 04ER86191, 04ER84016, 05ER86252, 05ER86253 and 06ER86282.

This was selected for an oral presentation.

b. Web Site:
http://www.muonsinc.com/

c. Networks or Collaborations Fostered:
We have been working with Fermilab experts on muon bunch coalescing (Ankenbrandt and Bhat) and experts on collider ring and interaction point design and simulations. The May 21-22, 2007 PIC/REMEX Workshop at Fermilab that has been organized by Muons, Inc. provided more opportunities to take advantage of Fermilab resources.

d. Technologies/Techniques:

The exposition of the physical foundations of PIC as seen in Appendix I has demonstrated that the technique should work. The helical solenoid approach may be the practical solution, but the simulations to show that are yet to be made.

e. Inventions/Patent Applications :

Most of Muons, Inc. inventions are particularly useful for large projects built by the US Government, which will have rights to our inventions as part of SBIR-STTR agreements. It is difficult to imagine commercially important applications for muon colliders in the time frame of a patent. We are pleased, however, to contribute to the progress toward the energy frontier, which has tremendous importance to humanity as a source of fundamental knowledge of our universe.

f. Other Products:

Related projects are described below on page 15.

Introduction and Background

Recently, several things have come together to reinvigorate muon collider enthusiasts: 1) There is a great interest to have a plan for a next-generation project that would continue the energy-frontier accelerator tradition in the US. 2) The uncertainties in need, cost, and siting of the International Linear Collider (ILC) have made it clear even to strong ILC supporters that a "Plan B" is prudent. 3) While impressive work has been done toward a neutrino factory based on a muon storage ring [9,10], the physics case for such a machine will have to wait for results of experiments that are just getting started. Thus there is some muon-related accelerator expertise that is available for muon collider development. 4) As discussed below, several new ideas have arisen in the last five years for six-dimensional (6D) muon beam cooling. The advantage of achieving high luminosity in a muon collider with beams of smaller emittance and fewer muons has been recognized as a great advantage for many reasons [11], including less proton driver power on target, fewer detector background issues, and relaxed site boundary radiation limitations.

Another advantage of small 6D emittance for a collider is that the cost of muon acceleration can be reduced by using the high frequency RF techniques being developed for the ILC. To the extent that muon beams can be cooled well enough, the muon collider is an upgrade path for the ILC if LHC results imply that the ILC energy is too low or if its cost is too great.

Effective 6D cooling and the recirculating of muons in the same RF structures that are used for the proton driver may enable a powerful new way to feed a storage ring for a neutrino factory [12]. This would put neutrino factory and muon collider development on a common path such that a muon collider could be realized in several stages, each independently funded and driven by high-energy physics goals.

A plan to achieve a Muon Collider in separately funded stages might involve the following steps:
1) An intense proton source like Project-X at Fermilab as an enabler for neutrino programs,
2) A very cool stopping muon beam for experiments such as mu2e,
3) A neutrino factory to study neutrino mixing parameters,
4) A Z' factory that requires a Muon Collider of modest luminosity, should such a particle be discovered at the LHC,
5) A Higgs factory with high luminosity but relatively lower energy,
6) And finally, an energy frontier Muon Collider.

Unlike electron-positron colliders, muon colliders do not have severe limitations due to synchrotron radiation at the collision point. Consequently, the muon collider could be further improved in energy and luminosity with better understanding and corresponding mitigation of neutrino-induced site boundary radiation limits. The present understanding of the site boundary radiation limitation indicates that a 4 TeV center of mass muon collider is possible at a site like Fermilab. Higher energies will require innovations and cleverness. However at the present time, a 4 TeV muon collider would be an excellent choice for a machine to surpass the effective energy of the LHC which is about 1.5 TeV. A muon collider option is even more attractive considering its excellent energy resolution that will allow needed precision measurements.

Ionization Cooling Principles

The idea that the transverse emittance of a beam could be reduced by passing it through an energy absorber originated in Novosibirsk many years ago [13,14]. Figure 1 is a schematic of the concept, showing how the angular divergence of a beam can be reduced.

Ionization cooling of a muon beam involves passing a magnetically focused beam through an energy absorber, where the muon transverse and longitudinal momentum components are reduced, and through RF cavities, where only the longitudinal component is regenerated. After some distance, the transverse components shrink to the point where they come into equilibrium with the heating caused by multiple coulomb scattering. The equation describing the rate of cooling is a balance between these cooling (first term) and heating (second term) effects:

$$\frac{d\varepsilon_n}{ds} = -\frac{1}{\beta^2}\frac{dE_\mu}{ds}\frac{\varepsilon_n}{E_\mu} + \frac{1}{\beta^3}\frac{\beta_\perp (0.014)^2}{2E_\mu m_\mu X_0} \quad . \qquad [1].$$

Here ε_n is the normalized emittance, E_μ is the muon energy in GeV, dE_μ / ds and X_0 are the energy loss and radiation length of the absorber medium, $\beta_\perp$ is the transverse beta-function of the magnetic channel, and β is the particle velocity. Muons passing through an absorber experience energy and momentum loss due to collisions with electrons. The derivations and discussions of the basic formulae of ionization cooling can be found in many places [15,16], where the energy loss is described by the Bethe-Bloch theory and the multiple-scattering heating is described by the Moliere theory [17].

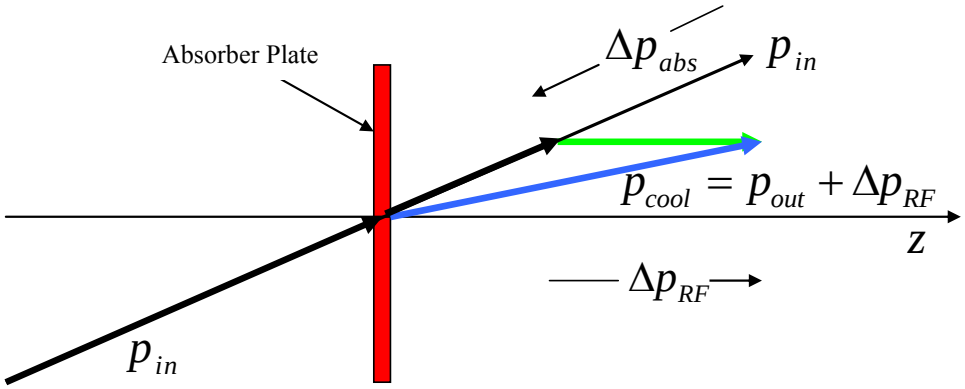

Figure 1: Conceptual picture of the principle of Ionization Cooling. Each particle loses momentum by ionizing an energy absorber, where only the longitudinal momentum is restored by RF cavities. The angular divergence is reduced until limited by multiple scattering, so that a low-Z absorber is favored.

Setting the heating and cooling terms equal defines the equilibrium emittance, the very smallest possible with the given parameters:

$$\varepsilon_n^{(equ.)} = \frac{\beta_\perp (0.014)^2}{2\beta m_\mu \frac{dE_\mu}{ds} X_0} \quad . \qquad [2].$$

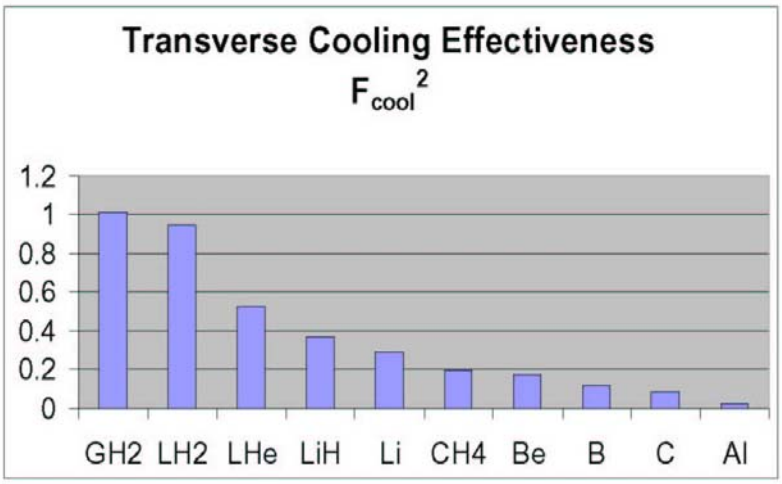

Figure 2: A comparison of the cooling figure of merit for light materials. The equilibrium beam emittance in each transverse plane is inversely proportional to the product of the energy loss and the radiation length. The graph indicates the total figure of merit.

A cooling factor ($F_{cool} = X_0 dE_\mu / ds$) can be uniquely defined for each material, and since cooling takes place in each transverse plane, the figure of merit is F_{cool}^2. For a particular material, F_{cool} is independent of density, since energy loss is proportional to density, and radiation length is inversely proportional to density. The inverse of F_{cool}^2 corresponds to the best equilibrium emittance that can be achieved. Super-conducting solenoidal focusing is used to give a value of $\beta_\perp$ as low as 10 cm. Figure 2 shows F_{cool}^2 for many materials of interest.

Gaseous hydrogen is the very best material that one can use from the standpoint of the final equilibrium emittance. Also, since the exponential cooling rate depends on the difference between the initial and final emittances, it provides the very best cooling rate.

Fundamental Limitations

The transverse beta function, $\beta_\perp$, is proportional to the ratio of momentum divided by the magnetic field. So the lowest equilibrium emittance requires the lowest momentum and the highest field.

As implied by the Bethe-Bloch equation and shown on figure 3, the fact that *dE/dx* increases as the momentum decreases means that once the momentum is below a few hundred MeV/c, any transverse cooling is necessarily accompanied by longitudinal heating. To a certain extent, this unwanted heating can be mitigated by modifying the dispersion function [18] and/or changing the profile of an absorber with shaped edges.

The maximum magnetic field is a technological problem that discussed below. One solution is the use of High Temperature Superconducting (HTS) magnets operating at low temperatures for large fields.

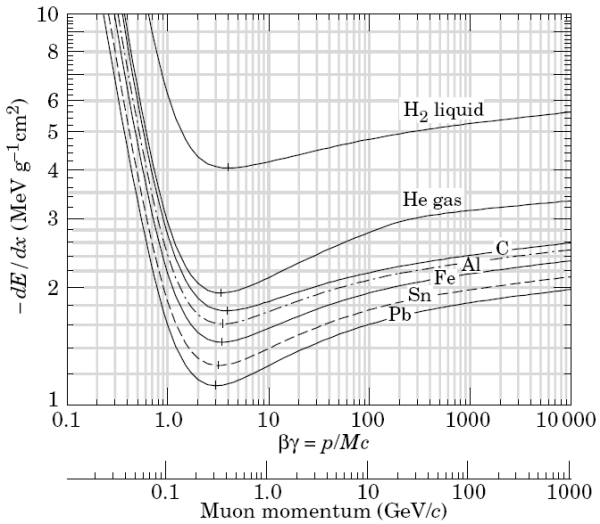

Figure 3: Energy loss for muons in various materials taken from the Particle Data Group [19], where the minimum dE/dx for hydrogen occurs near 300 MeV/c.

Multiple Scattering

Investigations of the deficiencies of the Moliere theory for low-Z materials [20] and other models [21] have been vindicated by recent measurements, as shown in figure 4. These seemingly small differences in the tails of the scattering distributions can have large consequences for long cooling channels. An ICOOL investigation indicated that as much as a factor of 3 improvement in cooling factor could be achieved with scattering models that agreed with the MuScat [22] data compared to the Geant4 models that we have used up to now.

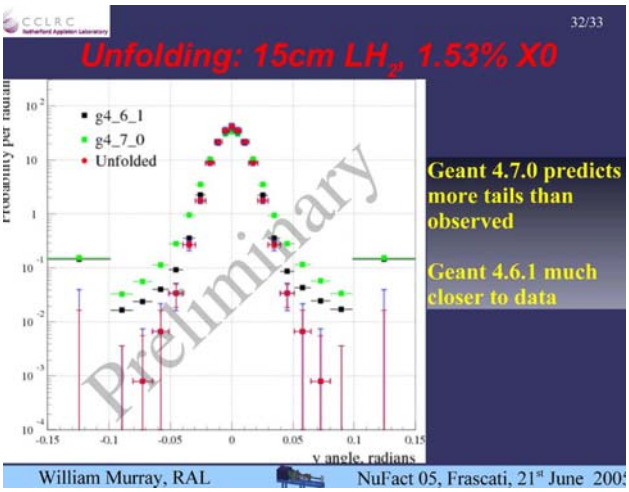

Figure 4: Comparison of angular distributions of the MuScat experiment for muons scattering off of hydrogen with two different releases of the Geant4 simulation program. The (red) experimental data show smaller tails.

Emittance Exchange

To achieve longitudinal cooling requires emittance exchange with transverse oscillations. Emittance exchange, in turn, requires the introduction of a beam bend that creates dispersion, a correlation between the orbit and energy of a particle. Figure 5 shows the conceptual pictures of

the two approaches that have recently been studied most. In the left of figure 5 the use of a wedge absorber is shown, where the beam is dispersed across a wedge of energy absorbing material such that higher momentum particles lose more energy. The muons become more monoenergetic after they pass through the wedge, while the transverse emittance is increased as part of the emittance exchange process.

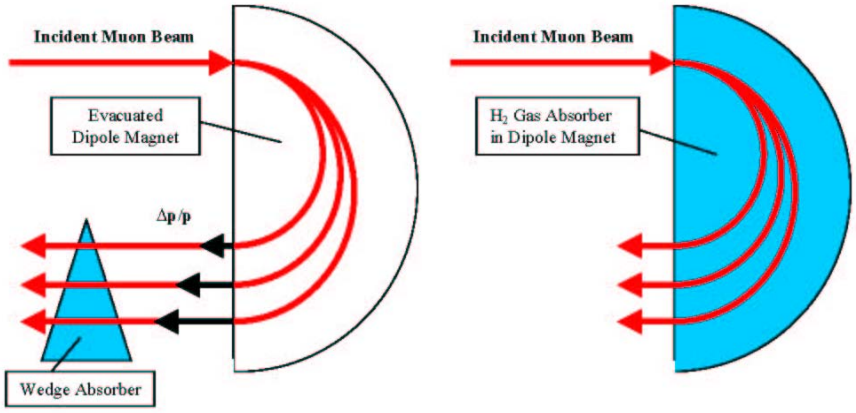

Figure 5: Emittance exchange. LEFT: Wedge Absorber Technique. RIGHT: Homogeneous Absorber Technique where dispersion causes higher energy particles to have longer path length and thus more ionization energy loss.

New Ionization Cooling Techniques

Gas-filled Helical Cooling Channel (HCC)

The HCC is an attractive example of a cooling channel based on this idea of energy loss dependence on path length in a continuous absorber. One version of the HCC uses a series of high-gradient RF cavities filled with dense hydrogen gas, where the cavities are in a magnetic channel composed of a solenoidal field with superimposed helical transverse dipole and quadrupole fields [23,24]. In this scheme, energy loss, RF energy regeneration, emittance exchange, and longitudinal and transverse cooling happen simultaneously.

The helical dipole magnet creates an outward radial force due to the longitudinal momentum of the particle while the solenoidal magnet creates an inward radial force due to the transverse momentum of the particle, or

$$\begin{aligned} F_{h-dipole} &\approx p_z \times B_\perp; \quad b \equiv B_\perp \\ F_{solenoid} &\approx -p_\perp \times B_z; \quad B \equiv B_z \end{aligned},$$

where B is the field of the solenoid, the axis of which defines the z axis, and b is the field of the transverse helical dipole at the particle position. By moving to the rotating frame of the helical fields, a time and z-independent Hamiltonian can be formed to derive the beam stability and cooling behavior [25]. The motion of particles around the equilibrium orbit is shown schematically in figure 6.

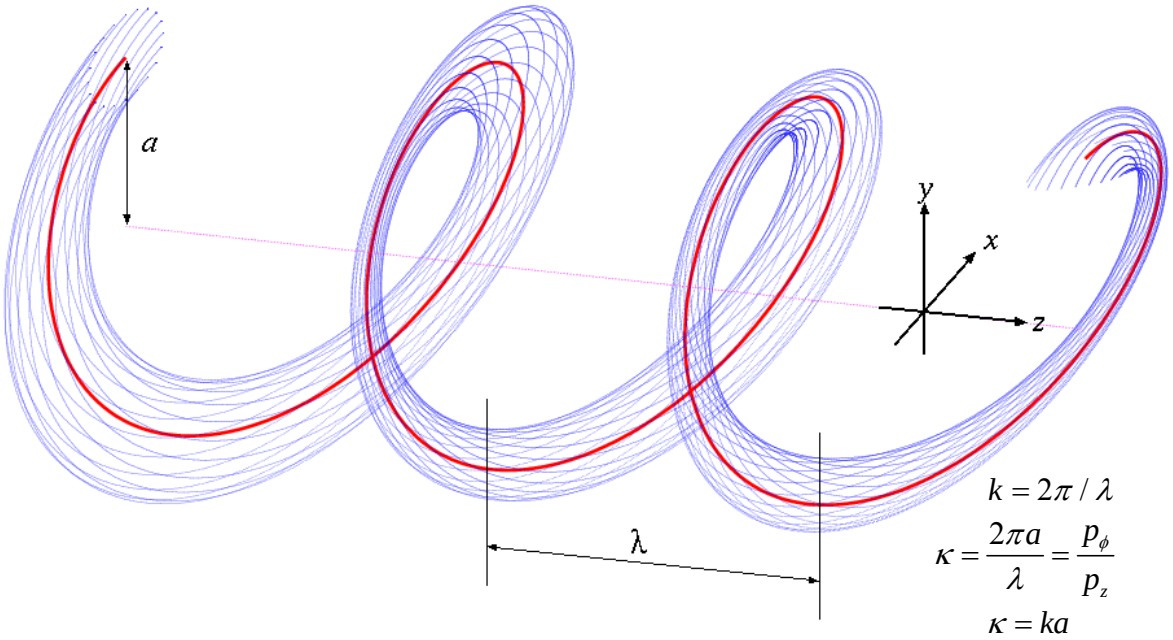

Figure 6: Schematic of beam motion in a helical cooling channel. The equilibrium orbit shown in red follows the equation that is the Hamiltonian solution:

$$p(a) = \frac{\sqrt{1+\kappa^2}}{k}\left[B - \frac{1+\kappa^2}{\kappa} b\right].$$

Use of a continuous homogeneous absorber as shown on the right side of figure 5, rather than wedges at discrete points, implies a positive dispersion along the entire cooling path, a condition that has been shown to exist for an appropriately designed helical dipole channel. We have also shown that this condition is compatible with stable periodic orbits. The simple idea that emittance exchange can occur in a practical homogeneous absorber without shaped edges followed from the observation that RF cavities pressurized with a low Z gas are possible [26,27].

The analytic relationships derived from this analysis were used to guide simulations using a code developed based on the GEANT4 [28] program called G4Beamline [29] and also using ICOOL [30] developed at BNL. Simulation results [18] show cooling factors or 50,000 for a series of 4 250 MeV/c HCC segments, where the magnet diameters are decreased and fields are increased as the beam cools. In this example the final field would be 17 T with a hydrogen gas pressure of 400 atmospheres.

Momentum-dependent HCC

While the HCC described above operates at constant energy, another set of applications follows from HCC designs where the strengths of the fields are allowed to change with the muon momentum. The first example was a 6D precooler, where the beam is slowed in a liquid hydrogen absorber at the end of the pion decay channel, with 6D emittance reduction by a factor of 6. The second example is the MANX six-dimensional cooling experiment discussed below. Another example is a stopping muon beam based on a HCC [31].

Reverse Emittance Exchange Using Absorbers

A muon beam that is well cooled at one or two hundred MeV/c will have its unnormalized longitudinal emittance reduced by a factor of a thousand or more at 100 or more GeV collider energy. At the interaction point in the collider the bunch length would then be much shorter than the IR focal length. In reverse emittance exchange (REMEX), we propose to repartition the emittances to lengthen each bunch and narrow the transverse emittances using beryllium wedge energy absorbers.

Calculations show that two stages of reverse emittance exchange, one at low energy and one at a higher energy before energy straggling becomes significant, can reduce each transverse emittance by an order of magnitude.

Muon Bunch Coalescing

One of the newest ideas is to cool less intense bunches at low energy and to recombine them into intense bunches at higher energy where wake fields, beam loading, and space charge tune shifts are less problematic [32]. Both PIC and REMEX techniques involve the focusing of a beam onto an energy absorber for which beryllium is better suited than the lower-Z materials shown in figure 2. First, the higher density of beryllium allows the thickness of the absorber to be a smaller fraction of a betatron wavelength and thereby more effective since the average betatron function in the region of the absorber is closer to the minimum value. Second, the energy straggling in the absorbers leads to longitudinal heating that must be controlled by emittance exchange. Thus the absorbers should be thin wedges made of beryllium which can easily be refrigerated to handle the heat deposition of the bright beams required by a muon collider.

Parametric Resonance Ionization Cooling

Parametric-resonance Ionization Cooling (PIC) [33], requires a half integer resonance to be induced in a ring or beam line such that the normal elliptical motion of particles in $x - x'$ phase space becomes hyperbolic, with particles moving to smaller x and larger x' as they pass down the beam line. (This is almost identical to the technique used for half integer extraction from a synchrotron where the hyperbolic trajectories go to small x' and larger x to pass the wires of an extraction septum.) Thin absorbers placed at the focal points of the channel then cool the angular divergence of the beam by the usual ionization cooling mechanism, where each absorber is followed by RF cavities. Thus in PIC the phase space area is reduced in x due to the dynamics of the parametric resonance and x' is reduced or constrained by ionization cooling. The basic theory of PIC is being developed to include aberrations and higher order effects. Simulations using linear channels of alternating dipoles, quadrupoles, solenoids, or HCC's are now underway [34]. The draft of the final paper on the PIC theory is presented in Appendix I and the significant results of simulations are shown in Appendix II (correction of chromatic aberrations using synchrotron motion), Appendix III (correction of spherical aberrations by channel symmetry), and Appendix IV (general optics criteria for PIC). Appendix V is the abstract of a paper to be presented at the European Particle Accelerator Conference in Genoa, Italy in June of 2008. The paper will contain the newest ideas on a way to create a beamline suitable for PIC that has a simple structure and homogeneous fields, but has a dispersion function that has the required characteristics.

Related Muons, Inc. Projects and Derivative Technologies

The projects discussed below are concerned with the production, cooling, and uses of intense and bright muon beams to be used for various purposes. These SBIR and STTR projects represent a coherent, innovative program to reduce the cost of neutrino factories, facilitate designs of high-intensity muon colliders, and provide muon beams with new physics potential.

Muons, Inc. started with the idea that a gaseous energy absorber enables an entirely new technology to generate high accelerating gradients for muons by using the high-pressure region of the Paschen curve [35]. This idea of filling RF cavities with gas is new for particle accelerators and is only possible for muons because they do not scatter as do strongly interacting protons or shower as do less-massive electrons. Additionally, use of a gaseous absorber presents other practical advantages that make it a simpler and more effective beam cooling method compared to liquid hydrogen flasks in the conventional designs.

Measurements by Muons, Inc. and IIT at Fermilab have demonstrated that hydrogen gas suppresses RF breakdown very well, about a factor six better than helium at the same temperature and pressure. Consequently, much more gradient is possible in a hydrogen-filled RF cavity than is needed to overcome the energy loss, provided one can supply the required RF power. Hydrogen is also twice as good as helium in ionization cooling effectiveness, and has better viscosity and heat capacity. For these reasons hydrogen is our material of choice.

As discussed below, recent measurements taken as part of the Phase I of this proposal show that hydrogen pressurized RF cavities do not suffer from a reduction in maximum gradient while operating in intense magnetic fields as do evacuated cavities. Thus it is possible to combine the energy absorber and RF reacceleration in pressurized cavities in regions where large magnetic fields create the required focusing for ionization cooling. This means that pressurized RF cavities have two very significant advantages over any scheme involving evacuated RF cavities: greater gradient in the required magnetic field and the simultaneous use of the hydrogen gas as energy absorber and breakdown suppressant. These two advantages each lead to shorter muon cooling channel designs, which minimize the loss of muons by decay and also lower construction costs.

The use of a continuous absorber as provided by a gas-filled RF system implies a new idea (first proposed as an SBIR topic) to provide a natural, very effective means of achieving emittance exchange and true six-dimensional (6D) cooling [36]. Namely, if the superimposed magnetic field provides dispersion down the beam channel such that higher momentum corresponds to longer path length and larger ionization energy loss, the momentum spread can be reduced. Simulations of a Helical Cooling Channel (HCC) of superimposed helical dipole, helical quadrupole, and solenoidal fields show a 6D emittance reduction by a factor of 50,000 in a channel only 160 meters long. This cooling factor is very much larger than in other cooling channels of comparable length.

Once the beam has been cooled in the HCC, other cooling techniques are possible. Recent developments have indicated that special cooling channels employing parametric resonances and/or very high field magnets can produce muon beams with small enough emittance that they

can be accelerated using 1.3 GHz RF cavities. Thus we have started thinking about a muon collider using superconducting RF technology as a possible upgrade to the International Linear Collider (ILC).

One possibility that was explored at the Low Emittance Muon Collider (LEMC) Workshops held at Fermilab (http://www.muonsinc.com/mcwfeb06/) Feb 6-10, 2006 and (http://www.muonsinc.com/mcwfeb07/) Feb 11-16, 2007 was to consider the proposed Fermilab 8 GeV superconducting proton driver Linac as a triple-duty machine on the path to an energy frontier muon collider. Such a Linac could accelerate protons to produce the muons, which would then be injected into the constant velocity section of the Linac to be accelerated by recirculation for use in a muon storage ring neutrino factory. (The third duty in this case would be to act as an ILC string test.) Such a neutrino factory could be very effective for two reasons. First, the neutrino production would scale with the repetition rate of the Linac and might easily outperform other designs. Second, the acceleration cost of the neutrino factory would be borne by the other uses of the superconducting Linac and the neutrino factory cost would be incremental. The present proposal is to explore ideas and techniques to capture and precool more muons so that this approach to a neutrino factory will be even more attractive.

The next step, first proposed under another SBIR grant (Reverse Emittance Exchange) with Thomas Jefferson National Accelerator Facility (JLab), described below, and explored at the first and second LEMC (http://www.muonsinc.com/mcwfeb07/) Feb 12-16, 2007 workshops, is to replace the muon storage ring of the neutrino factory with a coalescing ring to combine bunches for use in a muon collider. Such a muon coalescing ring could operate at the energy of the neutrino factory storage ring, above 20 GeV. The muon beam for the collider would then be similar to that of the neutrino factory up to the coalescing ring. This approach to a muon collider has several advantages that are very attractive. First, the development of the neutrino factory based on acceleration in the 1.3 GHz RF structures requires significant muon beam cooling so that the neutrino factory becomes an intermediate step to a collider. Second, the large single bunch intensities that a high luminosity muon collider requires are not needed at low energy where space-charge, wake fields, and beam loading are problematic.

Once the beam has been coalesced into a few high intensity bunches, recirculating Linacs using 1.3 GHz RF can accelerate them to a hundred GeV/c or more for a Higgs factory or to 2 to 3 TeV/c for an energy frontier muon collider. One of the studies of the present proposal will to be to investigate bunching techniques that are well suited for coalescing.

This path to an affordable neutrino factory and a compelling design of a muon collider has complementary projects that Muons, Inc. is pursuing with SBIR/STTR grants and proposals:

Phase II Projects

1) The development of Pressurized **High Gradient RF Cavities** was the subject of an STTR grant with IIT (Prof. Daniel Kaplan, Subcontract PI), which began in July 2002 and ended in September 2005. In this project, Muons, Inc. built two 805 MHz test cells (TC) and used them to measure the breakdown voltages of hydrogen and helium gases at FNAL with surface gradients up to 50 MV/m on copper electrodes. Phase II started in July 2003 to extend the measurements

at Fermilab's Lab G and the MuCool Test Area (MTA) to include effects of strong magnetic fields and ionizing radiation at 805 MHz. A new test cell was built under this grant, passed safety requirements associated with the high pressure hydrogen, and was used to extend Paschen curve measurements for hydrogen beyond 60 MV/m surface gradient (20μs pulse width) using electropolished molybdenum electrodes [37]. The new test cell is capable of 1600 PSI operation in the 5 Tesla LBL Solenoid, recently installed in the MTA, with ionizing radiation from the 400 MeV H^- Linac. IIT, Muons, Inc. and Fermilab staff members prepared a design [38] for a beam line from the Linac to the MTA using available magnets and other components, but the beam line is not expected to be completed until the end of 2008. We had planned to have a demonstration of pressurized high-gradient RF cavities operating in intense magnetic and radiation fields by the end of the STTR Phase II grant period, however the Lab G work was terminated when Fermilab operations removed the klystron from Lab G in January 2004. A klystron became available to us in the MTA in the summer of 2005 without the Solenoid or the implementation of the beam line. The Solenoid began operation in the MTA in March, 2006 and work on high-pressure RF cavities was restarted.

2) **Six-Dimensional (6D) Cooling** using gaseous absorber and pressurized high-gradient RF is the subject of an SBIR grant with Thomas Jefferson National Accelerator Facility (Dr. Yaroslav Derbenev, Subcontract PI), which began in July 2003 and ended in January 2007. A magnetic field configured such that higher energy particles have a longer path length can be used to generate the momentum-dependent energy loss needed for emittance exchange and six-dimensional cooling. In the 6D channel, helical dipole and solenoidal magnets and the RF cavities in them are filled with dense hydrogen so that higher energy particles then have more ionization energy loss. A paper describing the concepts and dynamics of this Helical Cooling Channel (HCC) grew out of the proposal for this grant and has been published in PRSTAB [25]. Recent simulations of a series of four such HCC segments have shown cooling factors of more than 50,000 in a 160 m long linear channel [39]. The 6D grant itself was to support the simulation of the channel by modifying existing computer codes and to optimize the design of the channel.

3) **Hydrogen Cryostat for Muon Beam Cooling** is an SBIR project begun in July 2004 and ended in January 2008 with Fermilab (Dr. Victor Yarba, Subcontract PI) to extend the use of hydrogen in ionization cooling to that of refrigerant in addition to breakdown suppressant and energy absorber. The project is to develop cryostat designs that could be used for muon beam cooling channels where hydrogen would circulate through refrigerators and the beam-cooling channel to simultaneously refrigerate 1) high-temperature-superconductor (HTS) magnet coils, 2) cold copper RF cavities, and 3) the hydrogen that is heated by the muon beam. In an application where a large amount of hydrogen is naturally present because it is the optimum ionization cooling material, it seems reasonable to explore its use with HTS magnets and cold, but not superconducting, RF cavities. However, the Helical Cooling Channel (HCC) cryostat developed in Phase I, because of new inventions, now has more variants than originally envisioned and there are now several cryostat designs to be optimized. In Phase I we developed computer programs for simulations and analysis and started experimental programs to examine the parameters and technological limitations of the materials and designs of HCC components (magnet conductor, RF cavities, absorber containment windows, heat transport, energy absorber, and refrigerant).

4) **Parametric-resonance Ionization Cooling (PIC)** is a project begun in July 2004 and ended in January 2008 with JLab as a research partner (Dr. Yaroslav Derbenev, Subgrant PI). The excellent 6D cooling expected from the SBIR Project 2 above leaves the beam with a small enough size and sufficient coherence to allow an entirely new way to implement ionization cooling by using a parametric resonance. The idea is to excite a half-integer parametric resonance in a beam line or ring to cause the usual elliptical motion on a phase-space diagram to become hyperbolic, much as is used in half-integer extraction from a synchrotron. This causes the beam to stream outward to large x' and/or y' while the spatial dimensions x and/or y shrink. Ionization cooling is then applied to reduce the x' and y' angular spread. The Phase II grant was to study the details of this new technique and to develop techniques for correction of chromatic and spherical aberrations and other higher-order effects using analytical calculations and numerical simulations.

5) Reverse Emittance Exchange (REMEX) for Muon Beam Cooling, with Jefferson Lab (Dr. Yaroslav Derbenev, Subgrant PI) is a Phase I STTR project begun in July 2005 to develop a technique to shrink the transverse dimensions of a muon beam to increase the luminosity of a muon collider. After the 6D cooling described in Project 2 above, the longitudinal emittance is small enough to allow high frequency RF for acceleration. However, the longitudinal emittance after the beam has been accelerated to collider energy is thousands of times smaller than necessary to match the beta function at the collider interaction point. We plan to repartition the emittances to lengthen the muon bunch and shrink the transverse bunch dimensions using linear cooling channel segments and wedge absorbers. A new concept of coalescing bunches to share longitudinal phase space with REMEX was developed in Phase I to enhance collider luminosity.

6) Muon Capture, Phase Rotation, and Precooling in Pressurized RF Cavities, with Fermilab (Dr. David Neuffer, Subgrant PI) begun in July 2005 has computational and experimental parts. The use of gas filled RF cavities close to the pion production target for phase rotation and beam cooling will be simulated. In parallel, the project will also involve a continuation of the experimental development in the Fermilab MuCool Test Area (MTA) of high-gradient high-pressure RF cavities operating in a high radiation environment and in strong magnetic fields.

7) Development and Demonstration of Six-Dimensional Muon Beam Cooling is with the Fermilab Technical Division (Dr. Rolland Johnson, PI, and Dr. Michael Lamm, subgrant PI). This project is to develop the MANX experiment to prove that effective 6D muon beam cooling can be achieved using an ionization-cooling channel based on a novel configuration of helical and solenoidal magnets. This Helical Cooling Channel (HCC) experiment is being designed with simulations and prototypes to provide an affordable and striking demonstration that 6D muon beam cooling is understood sufficiently well to become an enabling technology for intense neutrino factories and high-luminosity muon colliders. It is likely that the magnet system developed for this experiment could be used in **9)**, the stopping muon beam proposal now being considered for phase II funding.

8) Interactive Design and Simulation of Beams in Matter with IIT (Dr. Thomas J. Roberts, PI, Professor Daniel M. Kaplan, subgrant PI) is to develop G4BeamLine, a beam line design

program based on GEANT4 for beams with significant interactions with matter. G4BL has been the workhorse for Muons, Inc. and the International Muon Ionization Cooling Experiment (MICE) [40] collaboration to simulate muon cooling channels to explore new techniques. This project is to improve the program for more general use, adding a Graphical User Interface and several new and enhanced capabilities.

Phase I grants now being proposed for 2008 Phase II projects:

9) Stopping Muon Beams is a project with the Fermilab Accelerator Physics Center, (Dr. Rolland Johnson, PI and Dr. Charles Ankenbrandt, subgrant PI) to develop new techniques to capture and decelerate intense beams of muons for rare decay experiments, muon catalyzed fusion, and muon spin resonance uses. A key ingredient of the plan is to use a helical solenoid magnet as described below for this stopping muon beam application.

10) Magnets for Helical Cooling Channels is project to study the technology of the magnets that will be used for helical cooling channels with the Fermilab Accelerator Division (Dr. Rolland Johnson, PI, and Dr. Alexander Zlobin, subgrant PI).

11) Compact, Tunable RF Cavities is a project with the Fermilab Technical Division (Dr. Rolland Johnson, PI, and Dr. Milorad Popovic, subgrant PI) to develop new ideas for RF cavities that would be suitable for new applications such as Fixed Field Alternating Gradient Synchrotrons.

Work on these and other projects by Muons, Inc. and collaborators will be presented at EPAC08, where we have submitted 21 abstracts. To see them, go to
http://oraweb.cern.ch/pls/epac08/search.html
Enter the word “muons” in the affiliation field and hit search.

Although each of these projects is independent, taken together they represent a coherent plan to generate a compelling design for an intense muon source. The grants described above support over 14 FTE accelerator scientists. Muons, Inc. now has enthusiastic collaborators from the Illinois Institute of Technology, the Thomas Jefferson National Accelerator Facility, the Fermi National Accelerator Laboratory, Florida State University, the National High Magnetic Field Laboratory, Northern Illinois University, the University of Chicago, and Brookhaven National Laboratory who are part of this effort.

References

[1]Y. Derbenev and R.,P.,Johnson; Parametric-resonance Ionization Cooling and Reverse Emittance Exchange for Muon Colliders, COOL05 Presentation (2005)

Abstract: Two new ideas are being developed to reduce the transverse emittance of muon beams in order to increase the luminosity of muon colliders. The first idea involves driving a ½-integer parametric resonance in a beam line or ring such that particle motion becomes hyperbolic, where xx'=constant. With the proper phase of the resonance driving term, particles move to larger and larger x’ and smaller and smaller x at the position of a thin wedge absorber. The usual mechanism of ionization cooling reduces or constrains the excursion in x while the dynamics of

the resonance reduces the spread of x. The second idea takes advantage of the large reduction of relative momentum spread with increasing momentum in going from a few hundred MeV/c where the beam is cooled to a few TeV/c for an energy frontier collider. In this case we can use thin wedge absorbers to exchange the transverse and longitudinal emittances to make the transverse emittance smaller. These two ideas depend on careful control of the lattice functions and corrections for chromatic and spherical aberrations. We discuss these ideas and their potential luminosity implications considering the limitations of aberration corrections and of space charge effects.

[2] Y. Derbenev et al; Ionization Cooling Using a Parametric Resonance, PAC05.
Abstract: Muon collider luminosity depends on the number of muons in the storage ring and on the transverse size of the beams in collision. Ionization cooling as it is presently envisioned will not cool the beam sizes sufficiently well to provide adequate luminosity without large muon intensities. A new idea to combine ionization cooling with parametric resonances has been developed that will lead to beams with much smaller sizes so that high luminosity in a muon collider can be achieved with fewer muons. In the linear channel described here, a half integer resonance is induced such that the normal elliptical motion of particles in x-x' phase space becomes hyperbolic, with particles moving to smaller x and larger x' as they pass down the channel. Thin absorbers placed at the focal points of the channel then cool the angular divergence of the beam by the usual ionization cooling mechanism where each absorber is followed by RF cavities. We discuss the elementary theory of Parametric-resonance Ionization Cooling (PIC), including the need to start with a beam that has already been cooled adequately.

[3] PIC workshop directory: http://www.muonsinc.com/tiki-list_file_gallery.php?galleryId=12

[4] G4beamline access: http://www.muonsinc.com/tiki-index.php?page=Computer+Programs

[5] K. Beard et al; Simulations of Parametric Resonance Ionization Cooling of Muon Beams. PAC05
Abstract: Parametric-resonance ionization cooling (PIC) is being developed to create small beams so that high muon collider luminosity can be achieved with fewer muons. In the linear channel that is studied in this effort, a half integer resonance is induced such that the normal elliptical motion of particles in $x - x'$ phase space becomes hyperbolic, with particles moving to smaller x and larger x' as they pass down the channel. Thin absorbers placed at the focal points of the channel then cool the angular divergence of the beam by the usual ionization cooling mechanism where each absorber is followed by RF cavities. Thus the phase space of the beam is compressed in transverse position by the dynamics of the resonance and its angular divergence is compressed by the ionization cooling mechanism. We report the first results of simulations of this process, a study of the compensation of chromatic aberration by using synchrotron oscillations.
http://accelconf.web.cern.ch/AccelConf/p05/PAPERS/TPPP013.PDF

[6] David Newsham, Rolland Paul Johnson, Richard Sah (Muons, Inc, Batavia), S. Alex Bogacz, Yu-Chiu Chao, Yaroslav Derbenev (Jefferson Lab, Newport News, Virginia), PAC07, Simulations of Parametric-resonance Ionization Cooling,
http://pac07.org/proceedings/PAPERS/THPMN094.PDF

[7] R.P. Johnson, S.A. Bogacz, Y.S. Derbenev, Optics for Phase Ionization Cooling of Muon Beams, EPAC08, http://accelconf.web.cern.ch/AccelConf/e06/PAPERS/WEPLS018.PDF
Abstract: The realization of a muon collider requires a reduction of the 6D normalized emittance of an initially generated muon beam by a factor of more than 106. Analytical and simulation studies of 6D muon beam ionization cooling in a helical channel filled with pressurized gas or liquid hydrogen absorber indicate that a factor of 106 is possible. Further reduction of the normalized 4D transverse emittance by an additional two orders of magnitude is envisioned using Parametric-resonance or Phase Ionization Cooling (PIC). To realize the phase shrinkage effect in the parametric resonance method, one needs to design a focusing channel free of chromatic and spherical aberrations. We report results of our study of a concept of an aberration-free wiggler transport line with an alternating dispersion function. Resonant beam focusing at thin beryllium wedge absorber plates positioned near zero dispersion points then provides the predicted PIC effect.

[8] Andrei Afanasev, Yaroslav Derbenev, Rolland Johnson, Aberration-free Muon Transport Line for Extreme Ionization Cooling.
Abstract: Once the normalized transverse emittances of a muon beam have been cooled to some hundreds of microns, new techniques such as Parametric-resonance Ionization Cooling and Reverse Emittance Exchange can be used to focus the beam very tightly on beryllium energy absorbers for further transverse emittance reduction. The transport lines for these techniques have stringent requirements for the betatron tunes so that resonance conditions are properly controlled and for the dispersion function so that the longitudinal emittance can be controlled by emittance exchange using wedge-shaped absorbers. The extreme angular divergence of the beam at the absorbers implies large beam extension between the absorbers such that these techniques are very sensitive to chromatic and spherical aberrations. In this work we describe general and specific solutions to the problem of compensating these aberrations for these new muon cooling channels.

[9] http://www.fnal.gov/projects/muon collider/nu/study/report/machine report/

[10] http://www.cap.bnl.gov/mumu/studyii/FS2-report

[11] http://www.muonsinc.com/mcwfeb07

[12] M. Popovic et al., Linac06

[13] M. Ado, V. I. Balbekov, Sov. At. Energy 31, 731,'71

[14] A. N. Skrinsky and V. V. Parkhomchuk, Sov. J. Part. Nucl. 12, 223 (1981).

[15]D. M. Kaplan, http://www.slac.stanford.edu/ econf/C010630/papers/M102.PDF

[16] P. Gruber, CERN/NUFACT Note 023,
http://slap.web.cern.ch/slap/NuFact/NuFact/nf23.pdf

[17] Bethe, H. A.: Molière's Theory of Multiple Scattering, Phys Rev. **89**, 1256 (1953)

[18] K. Yonehara et al., EPAC06

[19] http://pdg.lbl.gov/2007/reviews/passagerpp.pdf

[20] A. V. Tollestrup & J. Monroe, MUCOOL note 176

[21] W. W. M. Allison et al.,
arxiv.org/PS_cache/physics/pdf/0609/0609195v1.pdf

[22] W. Murray, NuFact05, Frascati

[23] V. Kashikhin et al., Magnets for the MANX Cooling Demonstration Experiment, MOPAS012, PAC07

[24] S. A. Kahn et al., Magnet Systems for Helical Muon Cooling Channels, MOPAN117, PAC07

[25] Y. Derbenev and R. P. Johnson, Phys. Rev. Spec. Topics Accel. and Beams 8, 041002 (2005)

[26] R. P. Johnson et al., Linac04

[27] M. BastaniNejad et al.,RF Breakdown in Pressurized RF Cavities, WEPMS071, PAC07

[28] http://wwwasd.web.cern.ch/wwwasd/geant4/geant4

[29] T. J. Roberts et al., G4BL Simulation, PAC07

[30] R. Fernow, ICOOL, http://pubweb.bnl.gov/users/fernow/www/icool/readme.html

[31] M. A. C. Cummings et al., Stopping Muons Beams, THPMN096, PAC07

[32] C. M. Ankenbrandt et al., Muon Bunch Coalescing,, THMN095, PAC07

[33] Yaroslav Derbenev et al., COOL05

[34] D. Newsham et al., Simulations of PIC, PAC07

[35] Sanborn C. Brown, **Basic Data of Plasma Physics, The Fundamental Data on Electrical Discharges in Gases**, American Vacuum Society Classics, AIP Press, 1993.
http://home.earthlink.net/~jimlux/hv/paschen.htm

[36] Y. Derbenev and R. P. Johnson (Phys. Rev. Special Topics Accel. and Beams 8, 041002 (2005)) http://www.muonsinc.com/reports/PRSTAB-HCCtheory.pdf

[37] R. P. Johnson et al., LINAC2004, http://bel.gsi.de/linac2004/PAPERS/TU203.pdf

[38] http://www-mucool.fnal.gov/mcnotes/public/pdf/muc0287/muc0287.pdf

[39] Cool05 http://conferences.fnal.gov/cool05/Presentations/Tuesday/T09_Johnson.pdf

[40] http://hep04.phys.iit.edu/cooldemo/micenotes/public/pdf/MICE0021/MICE0021.pdf

PARAMETRIC-RESONANCE IONIZATION COOLING*

Yaroslav Derbenev, Jefferson Lab, Newport News, Virginia
Rolland P. Johnson#, Muons, Inc, Batavia, Illinois

Abstract

An idea to combine ionization cooling with parametric resonances has been developed that will lead to muon beams with much smaller transverse sizes so that high luminosity in a collider can be achieved with fewer muons. In the linear channel described here, a half integer resonance is induced such that the normal elliptical motion of particles in x-x' phase space becomes hyperbolic, with particles moving to smaller x and larger x' at the channel focal points. Thin absorbers placed at the focal points of the channel then cool the angular divergence of the beam by the usual ionization cooling mechanism where each absorber is followed by RF cavities. We discuss the theory of Parametric-resonance Ionization Cooling (PIC), starting with the basic principles in the context of a simple quadrupole-focused beam line. Then we discuss detuning caused by chromatic, spherical, and non-linear field aberrations and the techniques needed to reduce the detuning. We discuss the requirement that PIC be accompanied by emittance exchange in order to keep the momentum spread sufficiently small.

I. INTRODUCTION

Experiments at energy-frontier colliders require high luminosities, of order 10^{34} cm^{-2} sec^{-1} or more, in order to obtain reasonable rates for events having point-like cross sections. High luminosities require intense beams, small transverse emittances, and a small beta function at the collision point. For muon colliders, high beam intensities and small emittances are difficult and expensive to achieve because muons are produced diffusely and must be cooled drastically within their short lifetimes. Ionization cooling as it is presently envisioned will not cool the beam sizes sufficiently well to provide adequate luminosity without large muon intensities. However, to the extent that the transverse emittances can be reduced further than with conventional ionization cooling, several problems can be alleviated.

Lower transverse emittance allows a reduced muon current for a given luminosity, which implies:
1) a proton driver with reduced demands to produce enough proton power to create the muons;
2) reduced site boundary radiation limits from circulating muons that decay into neutrinos that interact in the earth;
3) reduced detector background from the electrons from the decay of circulating muons;
4) reduced proton target heat deposition and radiation levels;
5) reduced heating of the ionization cooling energy absorber;
6) less beam loading and wake field effects in the accelerating RF cavities.

Smaller transverse emittance has virtues beyond reducing the required beam currents, namely:
1) smaller, higher-frequency RF cavities with higher gradient can be used for acceleration;
2) beam transport is easier, with smaller aperture magnetic and vacuum systems;
3) stronger collider interaction point focusing can be used, since that is limited by beam extension in the interaction point (IP) quadrupoles.

Ionization cooling of a muon beam involves passing a magnetically focused beam through an energy absorber, where the muon transverse and longitudinal momentum components are reduced, and through RF cavities, where only the longitudinal component is regenerated. This is shown schematically in figure 1.

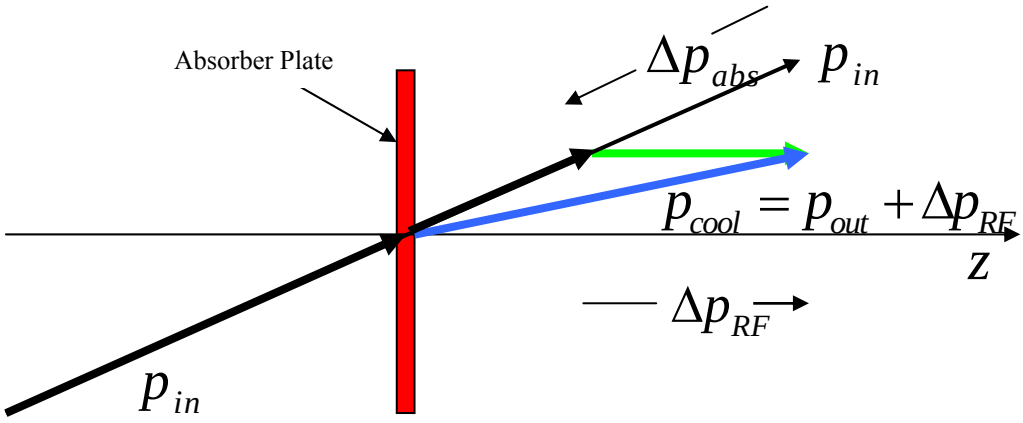

Fig. 1: Principle of transverse ionization cooling. A particle loses momentum in all three coordinates as it passes through an energy absorbing plate. Only the longitudinal component is replaced by RF fields, thereby reducing the angular divergence of the particle, $\vartheta = x'$.

After some distance, the transverse components shrink to the point where they come into equilibrium with the heating caused by multiple coulomb scattering. The equation describing the rate of cooling is a balance between these cooling (first term) and heating (second term) effects:

$$\frac{d\varepsilon_n}{ds} = -\frac{1}{v^2}\frac{dE_\mu}{ds}\frac{\varepsilon_n}{E_\mu} + \frac{1}{v^3}\frac{\beta(0.014)^2}{2E_\mu m_\mu X_0}.$$

Here ε_n is the normalized emittance, E_μ is the muon energy in GeV, dE_μ/ds and X_0 are the energy loss and radiation length of the absorber medium, $\beta = \lambda / 2\pi$ is the transverse beta-function of the magnetic channel, and v is the particle velocity normalized to light velocity.

Setting the heating and cooling terms equal defines the equilibrium emittance, the very smallest possible with the given parameters:

$$\varepsilon_n^{(equ.)} = \frac{\beta(0.014)^2}{2vm_\mu \frac{dE_\mu}{ds} X_0}.$$

One can see that the figure of merit for a cooling absorber material is the product of the energy loss rate times the scattering length. Up to now, liquid hydrogen has been the energy-absorbing medium of choice, with dE/ds= 60 MeV/m and X_0 = 8.7 m. Superconducting solenoidal focusing is used to give a small value of $\beta \sim 10$ cm, corresponding to a 100 MeV/c muon in a 6 T field.

In the PIC technique described below, the resonant approach to particle focusing can achieve equilibrium transverse emittances that are at least an order of magnitude smaller than in conventional ionization cooling. That is, the beam cooling in a conventional ionization cooling channel would require an unrealistically high magnetic field for an equilibrium transverse emittance as small as PIC can achieve. Another advantage to PIC is that a beryllium energy absorber is more effective than hydrogen, since the ratio of the absorber thickness to the betatron wavelength is a measure of its effectiveness. That is, the density of beryllium relative to hydrogen is more important than the product of energy loss rate times Coulomb scattering length in a channel that is required to be as short as possible to reduce losses by muon decay. The practical advantage of beryllium is that the required energy absorber geometry and refrigeration have straightforward engineering solutions.

II. BASIC PIC CONCEPTS

A. Hyperbolic dynamics of PIC

In general, a parametric resonance is induced in an oscillating system by using a perturbing frequency that is the same as or a harmonic of a parameter of the system. Physicists are often first introduced to this phenomenon in the study of a rigid pendulum, where a periodic perturbation of the pivot point can lead to stable motion with the pendulum upside down. Half-integer resonant extraction from a synchrotron is another example familiar to accelerator physicists, where larger and larger radial excursions of particle orbits at successive turns are induced by properly placed quadrupole magnets that perturb the beam at a harmonic of the betatron frequency. In this case, the normal elliptical motion of a particle's horizontal coordinate in phase space at the extraction septum position becomes hyperbolic, $xx' = const$, leading to a beam emittance which has a wide spread in x and narrow spread in x'.

In PIC, the same principle is used but the perturbation generates hyperbolic motion such that the emittance becomes narrow in x and wide in x' at certain positions as the beam passes down a line or circulates in a ring. Ionization cooling is then used to damp the angular spread of the beam. Figure 2 shows how the motion is altered by the perturbation. The principle of ionization cooling as described above is well known, where a particle loses momentum in all three coordinates as it

passes through some energy absorbing material and only the longitudinal component is replaced by RF fields. The angular divergence x' of the particle is thereby reduced until it reaches equilibrium with multiple Coulomb scattering in the material. The concept of ionization cooling is shown in figure 2.

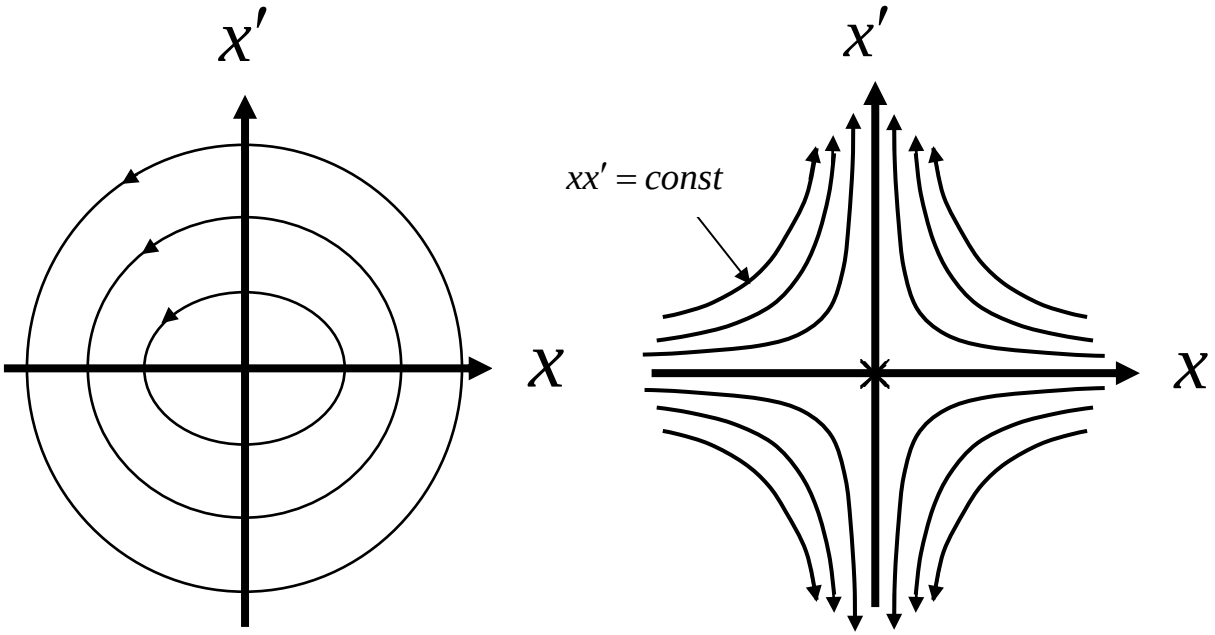

Fig. 2: Comparison of particle motion at periodic locations along the beam trajectory in transverse phase space for: LEFT ordinary oscillations and RIGHT hyperbolic motion induced by perturbations at a harmonic of the betatron frequency.

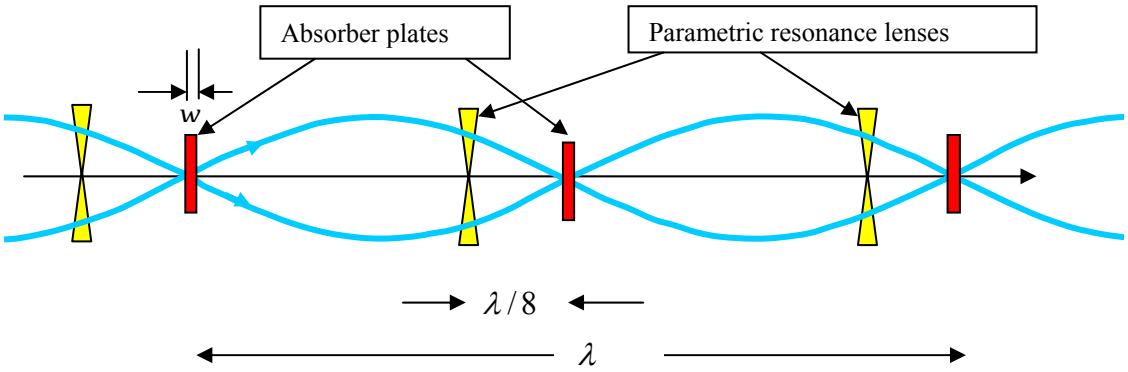

Fig. 3: Conceptual diagram of a beam cooling channel in which hyperbolic trajectories are generated in transverse phase space by perturbing the beam at the betatron frequency, a parameter of the beam oscillatory behavior. Neither the focusing magnets that generate the betatron oscillations nor the RF cavities that replace the energy lost in the absorbers are shown in the diagram. The blue trajectories indicate the betatron motion of particles that define the beam envelope.

Thus in PIC the phase space area is reduced in x due to the dynamics of the parametric resonance and x' is reduced or constrained by ionization cooling. For PIC to work, however, the beam must be cooled first by other means. For this analysis the initial conditions for PIC are assumed to be those as might be attained using a helical cooling channel [1] as shown in the table below.

Parameter	Unit	equilibrium rms value
Beam momentum, p	MeV/c	100
Synchrotron emittance, ε_s	μm	300
Relative momentum spread	%	2
Beam width due to $\Delta p / p$	mm	1.5
Bunch length	mm	11
Transverse emittances, $\varepsilon_+ / \varepsilon_-$	mm-mr	100/300
Beam widths, σ_1 / σ_2	mm	4.5/2.8

Table 1: Beam parameters after a proposed 6D helical cooling channel

Let there be a periodic focusing lattice of period λ along the beam path with coordinate z. Particle tracking or mapping is based on a single period transformation matrix, M (between two selected points, z_0 and $z_0 + \lambda$), for particle transverse coordinate and angle,

$$\begin{pmatrix} x \\ x' \end{pmatrix}_{z_0+\lambda} = M_x \begin{pmatrix} x \\ x' \end{pmatrix}_{z_0},$$

with a similar expression for the y coordinate.

The matrices M_x and M_y are symplectic or canonical, which means each has determinant equal to one. Otherwise, the matrix elements are arbitrary in general. Thus, each can be represented in a general form convenient for later discussions as follows:

$$M = \begin{pmatrix} e^{-\lambda\Lambda_d}\cos\psi & g\sin\psi \\ -\frac{1}{g}\sin\psi & e^{\lambda\Lambda_d}\cos\psi \end{pmatrix}. \quad (1)$$

In particular, the optical period can be designed such that, for $\sin\psi = 0$ (i.e. $\psi = \pi$ or $\psi = 2\pi$), the evolving particle coordinate and angle (or momentum) appear uncoupled:

$$(x)_{z_0+\lambda} = \pm e^{-\lambda\Lambda_d}(x)_{z_0} \text{ and } (x')_{z_0+\lambda} = \pm e^{\lambda\Lambda_d}(x')_{z_0}.$$

Thus, if the particle angle at point z_0 grows ($\Lambda_d > 0$), then the transverse position experiences damping, and vice versa. Liouville's theorem is not violated, but particle trajectories in phase space are hyperbolic ($xx' = const$); this is an example of a parametric resonance. Exactly between the two resonance focal points the opposite situation occurs where the transverse particle position grows from period to period, while the angle damps.

B. Stabilizing absorber effect

If we now introduce an energy absorber plate of thickness w at each of the resonance focal points as shown in figure 3, ionization cooling damps the angle spread with a rate Λ_c. Here we assume balanced 6D ionization cooling, where the three partial cooling decrements have been equalized using emittance exchange techniques as described in reference [1]:

$$\Lambda_c = \frac{1}{3}\Lambda, \quad \Lambda = 2\frac{\langle \gamma'_{abs} \rangle}{\gamma} = 2\frac{\gamma'_{acc}}{\gamma}, \quad \langle \gamma'_{abs} \rangle = \gamma'_{abs} 2w/\lambda,$$

where γ'_{abs} and γ'_{acc} are the intrinsic absorber energy loss and the RF acceleration rates, respectively. If $\Lambda_d = \Lambda_c / 2$ then the angle spread and beam size are damped with decrement $\Lambda_c / 2$:

$$\begin{pmatrix} x \\ x' \end{pmatrix}_{z_0+\lambda} = e^{-\lambda\Lambda_c/2} \begin{pmatrix} x \\ x' \end{pmatrix}_{z_0}.$$

C. Reduction of phase diffusion and equilibrium emittance

The rms angular spread is increased by scattering and decreased by cooling,

$$\frac{d}{dz}\overline{(x')^2} = \frac{(Z+1)}{2\gamma v^2}\frac{m_e}{m_\mu}\Lambda - \Lambda_c \overline{(x')^2},$$

which leads to the equilibrium angular spread at the focal point:

$$\overline{(x')^2_{eq}} = \frac{1}{\Lambda_c}\frac{d}{dz}\overline{(x')^2_{z_0}} = \frac{3}{2}\frac{(Z+1)}{\gamma v^2}\frac{m_e}{m_\mu}. \tag{2}$$

The rms product $\left[\overline{(x^2)}\cdot\overline{(x')^2}\right]^{\frac{1}{2}}_{z_0}$ determines the effective 2D beam phase space volume, or emittance.

Taking into account the continuity of x in collisions, the diffusion rate of particle position at the focus is a function of $s = z - z_0$, the local position of the beam within the absorber:

$$\delta(x)_{z_0} = -s\delta x', \quad -\frac{w}{2} \le s \le \frac{w}{2},$$

$$\frac{d}{dz}\overline{(\delta x)^2_{z_0}} = \frac{w^2}{12}\frac{d}{dz}\overline{(\delta x')^2}. \tag{3}$$

Thus, in our cooling channel with resonance optics and correlated absorber plates, the equilibrium beam size at the plates is determined not by the characteristic focal parameter of the optics, $\lambda/2\pi$, but by the thickness of absorber plates, w. Hence, the equilibrium emittance is equal to

$$(\varepsilon_x)_{eq} = \gamma v\left[\overline{(x^2)}\cdot\overline{(x')^2}\right]^{\frac{1}{2}}_{z_0} = \gamma v\frac{w}{2\sqrt{3}}\overline{(x')^2_{z_0}} = \frac{\sqrt{3}}{4v}(Z+1)\frac{m_e}{m_\mu}w.$$

The emittance reduction by PIC is improved compared to a conventional cooling channel by a factor

$$\frac{\pi}{\sqrt{3}}\frac{w}{\lambda} = \frac{\pi}{2\sqrt{3}}\frac{\gamma'_{acc}}{\gamma'_{abs}}.$$

Using the well-known formula for the instantaneous energy loss rate in an absorber, we find an explicit expression for the transverse equilibrium emittance that can be achieved using PIC:

$$\varepsilon_x = \frac{\sqrt{3}}{16} v \left(1 + \frac{1}{Z}\right) \frac{(\lambda/2\pi)}{n r_e^2 \log} \gamma'_{acc}.$$

Here Z and n are the absorber atomic number and concentration, r_e the classical electron radius, and v is the muon velocity. Here log is a symbol for the Coulomb logarithm of ionization energy loss for fast particles:

$$\log \equiv \ln\left(\frac{2p^2}{h\nu\, m_\mu}\right) - v^2,$$

with m_μ the muon mass and $h\nu$ the effective ionization potential [2]. A typical magnitude of the log is about 12 for our conditions. The equilibrium emittance in the resonance channel is primarily determined by the absorber atomic concentration, and it decreases with beam energy in the non-relativistic region.

III. COMBINING PIC WITH EMITTANCE EXCHANGE

Longitudinal cooling must be used with PIC in order to maintain the energy spread at the level achieved by the basic 6D cooling from the helical cooling channel. Emittance exchange must therefore be used for longitudinal cooling, which requires the introduction of bends and dispersion. Since the beam has already undergone basic 6D cooling, its transverse sizes are so small that the absorber plates can have a large wedge angle to provide balanced 6D cooling even with small dispersion. Since the beam size at the absorber plates decreases as it cools, the wedge angle can increase along the beam path while the dispersion decreases. In this way, longitudinal cooling is maintained while the straggling impact on transverse emittance is negligible. Thus there is no conceptual contradiction to have simultaneous maximum transverse PIC with optimum longitudinal cooling.

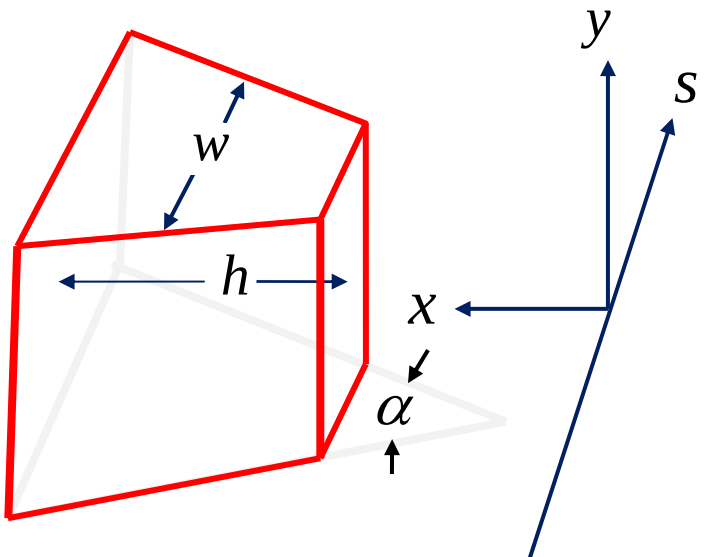

Fig. 4: Geometry of a wedge-shaped absorber. The average thickness of the absorber in the beam (s) direction is w. In this diagram, the magnetic field of the dipoles of the channel is along the y axis such that the dispersion is in the x direction, where h is the horizontal size of the absorber in the x direction. The wedge angle α is determined by the requirement that emittance exchange and longitudinal cooling must accompany PIC to keep the energy spread small to control chromatic detuning.

A. Emittance exchange using wedge absorbers

In order to prevent energy spread growth in the beam due to energy straggling in the absorber, one can use wedge absorber plates and introduce dispersion, i.e. make the beam orbit energy-dependent. Such dependence results from a beam bend by a dipole field (alternating along the beam line). As usual, the particle coordinate relative to a reference orbit can be represented as a superposition

$$x = D\frac{\Delta\gamma}{\gamma v^2} + x_b \tag{4}$$

where the dispersion D and x_b do not interfere on the particle trajectory. The absorber wedge orientation (i.e. the gradient of the plate width) must alternate coherently with the D oscillation. Considering only the effects of energy loss in the wedge absorber plates, we find a systematic change of particle energy and position x_b at the plates:

$$\Delta\gamma' = \frac{\partial\gamma'}{\partial\gamma}\Delta\gamma + \frac{\partial\gamma'}{\partial x}x = \frac{\Lambda}{2v^2}(\frac{2}{\gamma^2} - \frac{D_a}{h}\Delta\gamma)$$

$$(x_{0b}^2)' = -2(\Lambda_d - \frac{\Lambda}{2v^2}\frac{D_a}{h})x_{0b}^2.$$

Here we introduced the parameter h as an effective height of the absorber wedge as indicated in figure 4:

$$h^{-1} = \frac{1}{\gamma'}\frac{\partial\gamma'}{\partial x},$$

and D_a, the dispersion at the absorber plates. Thus, if the ratio D_a / h is positive, there is damping of the energy spread while the phase cooling decrement decreases. Let us assume an arrangement that makes the decrements of the three emittances equal to $\Lambda/3$ yet leaves equal the damping decrements of beam size and angle spread at the absorber plates. This assumption leads to the following relationships:

$$D_a = 2h(1 - \frac{2}{3}v^2) \equiv D_o\,. \tag{5}$$

IV. PIC FOR AN IDEALLY TUNED BEAM

A. Transverse equilibrium

The dispersion introduced for longitudinal cooling will also cause transverse emittance growth because of straggling, the stochastic change of particle energy due to scattering off of electrons in the absorber [3]. The related change of the particle 'free' coordinate x_b after scattering in a plate can be found simply taking again into account the continuity of the total coordinate x:

$$D_0\frac{\delta\gamma}{\gamma v^2} + \delta x_b = 0.$$

Thus we find the betatron coordinate diffusion rate due to energy straggling:

$$\frac{d}{ds}\overline{(\delta x_b)^2_{str}} = \frac{1}{2}\overline{\frac{D^2}{\gamma^2 v^4}\frac{d}{ds}(\delta\gamma)^2} = \frac{\Lambda}{8}\frac{\gamma^2+1}{\gamma v^2\log}\frac{m_e}{m_\mu}D_a{}^2\,.$$

Combining this with the angle scattering in equation (3), we obtain the total rate of betatron coordinate diffusion and the associated beam size at the absorber plate and the emittance:

$$\overline{(x_b^2)'} = \frac{\Lambda}{8\gamma\beta^2}\frac{m_e}{m_\mu}\left[\frac{Z+1}{3}w^2 + \frac{\gamma^2+1}{\log}4h^2(1-\frac{2}{3}v^2)^2\right]$$
$$\sigma_b^2 = \frac{1}{8\gamma v^2}\frac{m_e}{m_\mu}[(Z+1)w^2 + 12\frac{\gamma^2+1}{\log}h^2(1-\frac{2}{3}v^2)^2] \quad (6)$$
$$\varepsilon_{eq} = \varepsilon_0 \equiv \gamma v \vartheta_0 \sigma_0$$

The contribution of straggling to transverse emittance growth can be minimized by reducing the wedge absorber horizontal size h. However h must be large compared to σ_b. Let us introduce $\chi_h = \sigma_b / h$, then equation (6) can be written:

$$\sigma_b^2 = \frac{Z+1}{8\gamma v^2}\frac{m_e}{m_\mu}w^2\frac{1}{1-\frac{3}{2\chi^2 v^2}\frac{m_e}{m_\mu}\frac{\gamma^2+1}{\gamma\log}(1-\frac{2}{3}v^2)^2}$$

The condition for straggling not to be important is

$$1 >> \chi >> (1-\frac{2}{3}v^2)[\frac{3}{2v^2}\frac{\gamma^2+1}{\gamma\log}\frac{m_e}{m_\mu}]^{1/2}$$

B. Optimum cooling and PIC equilibrium

We define optimum cooling by equating the three emittance cooling rates (thus, making each of them equal to $\Lambda/3$) to obtain the following relationships:

$$\frac{D}{h} = 2-\frac{4}{3}v^2; \quad \frac{\Lambda_d}{\Lambda} = \frac{1}{2v^2}-\frac{1}{6} \quad (7)$$

Then the balance equations lead to equilibrium as follows:

$$\theta^2 = \frac{3m_e}{2\gamma v^2 m_\mu}(Z+1+\frac{\gamma^2+1}{4\log}D'^2) \quad (8)$$

$$\sigma^2 = \frac{3m_e}{2\gamma v^2 m_\mu}(\frac{Z+1}{12}w^2 + \frac{\gamma^2+1}{4\log}D^2) \quad (9)$$

$$(\frac{\Delta p}{p})^2 = \frac{3m_e}{8\gamma v^2 m_\mu}\cdot\frac{\gamma^2+1}{\log}.$$

For the conditions that follow from equations (8) and (9),

$$D' << 2\left(\frac{Z+1}{\gamma^2+1}\log\right)^{1/2} \text{ and } h \ll \frac{w}{(1-\frac{2}{3}v^2)}\left[\frac{(Z+1)\log}{12(\gamma^2+1)}\right]^{1/2},$$

the equilibrium normalized transverse emittance and beam size σ will be close to minimum values:

$$\varepsilon_\perp \Rightarrow \varepsilon_{\perp 0} = \frac{\sqrt{3}}{4v}(Z+1)\frac{m_e}{m_\mu}w, \ \sigma = \frac{\theta w}{2\sqrt{3}} \tag{10}$$

.

C. PIC potential

Table 1: Potential PIC effect

Parameter	*Unit*	*Initial*	*Final*
Beam momentum, p	MeV/c	100	100
Distance between plates, $\lambda/2$	cm	19	19
Plate thickness, w	mm	6.4	1.6
Intrinsic energy loss rate (Be)	MeV/m	600	600
Average energy loss	MeV/m	20	5
Angle spread at plates, rms, $\theta_x = \theta_y$,	mr	150	200
Beam transverse size at plates, rms, $\sigma_x = \sigma_y$	mm	2.0	0.1
Transverse rms emittance, norm. $\varepsilon_x = \varepsilon_y$	μm	300	20
Momentum spread , $\Delta p / p$, rms	%	2.7	2.7
Bunch length σ_z, rms	cm	1	1
Longitudinal emittance $\sigma_z \Delta p / mc$	cm	$2.7\text{x}10^{-2}$	$2.7\text{x}10^{-2}$
PIC channel length	m	100	
Integrated energy loss	GeV	0.7	
Beam loss due to muon decay	%	15	
Number of particles/bunch		10^{11}	
Tune spread due to space charge*, $\Delta\lambda/\lambda$	.001	0.75	

*To overcome the space charge impact on tuning, one can implement a beam recombining scheme: generate a low charge/bunch beam and recombine bunches after cooling and acceleration to sufficiently relativistic energy [4].

The equilibrium emittance (5) can be expressed as function of the intrinsic energy loss in the absorber, E_i' and the average energy loss or accelerating field using the relationships $(2w/\lambda)E_i' =< E_i' >=< E_{acc}' >$:

$$\varepsilon_{\perp 0} = \frac{\sqrt{3}}{8v}\frac{m_e}{m_\mu}\lambda\frac{< E_i' >}{E_i'}(Z+1).$$

The emittance that can be achieved after an "ordinary" (non-resonance) 6D cooling [1] in hydrogen absorber is $\varepsilon_{ord} = (3\lambda m_e / 2\pi v m_\mu)$; so PIC results in the reduction of transverse emittance by a factor $\frac{\pi}{4\sqrt{3}}\frac{< E_i' >}{E_i'}(Z+1)$. The factor $E_i'/(Z+1)$ is about $(60/v^2)$ MeV/m in the case of beryllium (compare with $15/v^2$ MeV/m in the case of liquid hydrogen) and does not change significantly with Z for heavier elements. Note that use of absorbers with large atomic number is disadvantageous because of the small thickness of the plates, which makes it difficult to tune to resonance. Note also that the equilibrium emittance can be decreased by decreasing the plate thickness and lowering the accelerating field, which makes the beam line longer. Thus the cooling rate and equilibrium emittance are limited by beam loss due to muon decay. For an optimal PIC design, the plate thickness *w* should diminish along the cooling channel, starting from a maximum determined by the available accelerating voltage. Table 1 illustrates the PIC effect.

V. TUNING DEMANDS OF PIC

For PIC to work at all, the relative spread in betatron function must be much smaller than the ratio of the betatron function to the cooling length, $l_c = \gamma mc^2 / < E' >$:

$$\frac{\Delta\beta}{\beta} << \frac{\beta}{l_c}.$$

The phase advance accumulated along a single cooling decrement length must be smaller than the absorber thickness divided by the beta function in order for PIC to work with full efficiency:

$$\delta\psi = \int_{l_c}\frac{\delta\beta(s)}{\beta^2}ds << \frac{w}{\beta}.$$

The precision required to control elements for compensating spherical and chromatic aberrations is

$$\frac{w}{l_c}\frac{\beta}{\Delta\beta}.$$

Random linear optics errors lead to a requirement for beta function control:

$$\frac{\Delta\beta}{\beta} << \frac{w}{l_c}\sqrt{\frac{l_c}{\beta}}.$$

VI. SNAKE CHANNEL FOR PIC

A. Alternating dispersion and linear optics design

The main constraint of parametric resonance ionization cooling channel design is to combine low dispersion at the wedge absorber plates (for emittance exchange to compensate energy straggling) with large dispersion in the space between plates (where sextupoles can be placed to compensate for chromatic aberration). This constraint can be achieved in a channel created by a "snake channel" which has an alternating dipole field as indicated in figure 5.

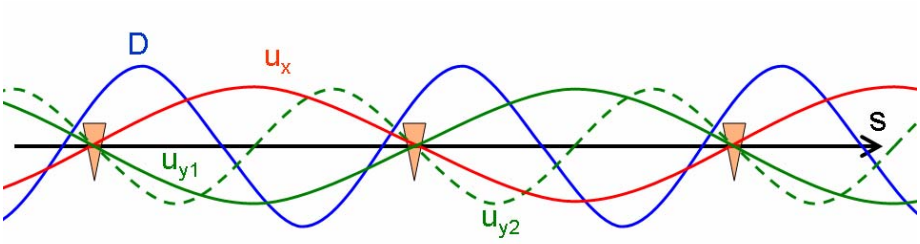

Fig. 5: Lattice functions of a beam cooling channel suitable for PIC showing D, the dispersion (blue), the horizontal betatron amplitude u_x (red), and two possible solutions for the vertical betatron amplitude, u_{y1} and u_{y1} (green). The triangles represent the wedge absorbers. The dipoles and quadrupoles are not shown.

In such a channel, the dispersion alternates with the orbit displacement. The absorber plates then are positioned near zero dispersion points. Obviously, the betatron (i.e. focusing) wave length must not be the same as the bend and dispersion periods, but it can be two or four times longer. Thus one should design the alternating bend, non-coupled linear optics channel such that the dispersion and wedges maintain the minimum momentum spread (~2.5%) and that the dispersion is small enough at the absorbers to prevent a *straggling impact* on the horizontal emittance, but large in between to compensate for *chromatic detuning.*

The notation for the following discussion follows the normal conventions:

$$x'' + (K^2 - n)x = K\Delta p;$$

$$y'' + ny = 0$$

$$x = D\frac{\Delta p}{p} + \tilde{x}$$

$$D'' + (K^2 - n)D = K$$

$$\tilde{x}'' + (K^2 - n)\tilde{x} = 0$$

Three possible cases suitable for PIC are:

$$\lambda_x = \lambda_y \qquad (K^2 - n \approx n)$$

$$\lambda_x = 2\lambda_y \qquad (K^2 - n \approx \frac{n}{4})$$

$$\lambda_y = 2\lambda_x \qquad (K^2 - n = 4n)$$

To avoid resonance between the dispersion and horizontal betatron motion, the dispersion period λ_0 must be half or one quarter of λ_x.

It is convenient to use a symmetric lattice to simplify the linear optics design and the addition of aberration correction elements. The symmetry relative to the absorbers can be chosen naturally with *K* and *D* antisymmetric and K^2 and *n* symmetric. Note that *D* is not exactly antisymmetric since some small dispersion is needed at the absorbers in order to create the emittance exchange required for longitudinal cooling.

Since the lattice we need is designed with correlated dispersion and betatron motion, we are sensitive to unwanted strong linear structure parametric resonances that must be avoided. The desired driving parametric resonance can be arranged in two planes by modulation of *B* and *n*.

B. Parametric resonance in the snake channel

Here we derive the equations for a perfectly tuned snake channel with no tune spread. Consider motion in the horizontal plane:

$$x'' + k^2(1 - 2\zeta \sin 2kz)x = 0 \ , \tag{11}$$

where $\zeta = const << 1$ is the frequency modulation parameter. Let us represent the oscillator motion in terms of "slow" variables $a(z), b(z)$ that would be constant at $\zeta = 0$:

$$\begin{aligned} x &= a\cos kz + b\sin kz \\ x' &= -ak\sin kz + bk\cos kz \ . \end{aligned} \tag{12}$$

Apparently, a and kb represent particle coordinate and angle in the x-plane, respectively, at points of the beam orbit where $\sin kz = 0$, while at points where $\cos kz = 0$ the coordinate and angle are correspondently represented by b and ka. Let us rewrite relationships (12) using the variables a and b as functions of x and x':

$$\begin{aligned} a &= x\cos kz - (x'/k)\sin kz \\ b &= x\sin kz + (x'/k)\cos kz \ . \end{aligned} \tag{13}$$

Then, we can easily find the derivatives a' and b' by taking into account the equation of motion for $x(z)$:

$$\begin{aligned} a' &= -2k(\zeta \sin 2kz)x\sin kz \\ &\equiv -2k(\zeta \sin 2kz)(a\cos kz + b\sin kz)\sin kz \\ b' &= 2k(\zeta \sin 2kz)x\cos kz \\ &\equiv 2k(\zeta \sin 2kz)(a\cos kz + b\sin kz)\cos kz \ . \end{aligned} \tag{14}$$

Thus, we derived the equations of motion in terms of slow variables a and b. The coefficients of these equations are periodic with period π / k. Assuming that both parameters ζ and ν are small, we can approximate the change of a and b during a single period by simply integrating the equations over one period at a =const, b = const on the right side of the equations. Then we find:

$$\begin{aligned} \Delta a &= -(\pi/2)(\zeta a) \\ \Delta b &= \ (\pi/2)(\zeta b) \end{aligned} \ ,$$

or, in terms of the effective differential equations,

$$a' \equiv (k/\pi)\Delta a = -(\zeta/2)ka$$
$$b' \equiv (k/\pi)\Delta b = \quad (\zeta/2)kb$$

These equations can also be obtained by an immediate averaging of equations (14) over z.

Assume now for certainty $\zeta > 0$. According to these equations the beam experiences an exponential shrinkage at points where $\sin kz = 0$, where we can put absorbers. The angle spread would grow exponentially if it were not constrained by the ionization cooling due to the absorber. Correspondently, the beam size grows while angle spread damps at points $\cos kz = 0$. Thus, at the exact parametric resonance we observe the hyperbolic dynamics identical to that described in section II above. It is possible to have the same resonant condition in the vertical plane such that the beam will be focused simultaneously at the same point in both planes.

VII. SNAKE CHANNEL WITH COUPLING RESONANCE

In order to cool in both transverse planes, one could alternate PIC sections with vertical or horizontal dispersion. Another possibility that could be more convenient would be to introduce a coupling resonance as a way to equalize the cooling rates in each transverse plane and to simplify the parametric resonance design by using skew-quads. It is critically important to design the two betatron periods to be different by a factor of 2 so that the coupling resonance causes beam rotation in space at the absorber, while keeping the horizontal and vertical beam sizes small and maintaining the PIC condition. The skew gradient field should alternate with a frequency equal to the difference of the two betatron frequencies. The effective Hamiltonian of the skew lattice can be represented as

$$H_c = gxy \sin\frac{k_0}{2}s = gxy\sin(k_x - k_y)s\,,$$

with constant parameter, g. By applying an averaging method to the equations of x and y motion in terms of slow variables a and b as above used in the case of the parametric resonance, we obtain the coupled x-y dynamics with equations as follows:

$$a_x' = \frac{g}{4}a_y \quad b_x' = \frac{g}{4}b_y$$
$$a_y' = -\frac{g}{4_y}a_x \quad b_y' = -\frac{g}{4}b_x\,.$$

The equations show that the coupling resonance causes beam rotation at the absorbers (where the beam is focused by the parametric resonance), while it does not change the sum of the Courant-Snyder actions. If the coupling parameter g is large enough compared to the rates of the parametric resonance and ionization cooling, the coupling resonance will effectively equalize the PIC dynamics and cooling rates of the two planes.

Another important attribute of the coupling resonance is that it also can be effectively used to reduce the number of compensation conditions for detuning due to numerous chromatic, geometrical, and non-linear aberrations in the optics of the PIC channel. This reduction becomes critical while approaching equilibrium at the end of the PIC process.

VIII. COMPENSATION FOR ABERRATIONS

The realization of Parametric-resonance Ionization Cooling requires compensation for tune spreads caused by numerous aberrations: chromatic, spherical, and non-linear field effects. Our analysis of the compensation is based on the expansion of the Hamiltonian function for a planar snake type beam transport derived in the Appendix.

A. Compensation for Chromatic Aberrations

The chromatic terms to be compensated are seen in the third power terms of the expansion of the Hamiltonian:

$$H_3 = -\frac{1}{2}(p_x^2 + p_y^2)(q - Kx) - \frac{1}{2}K[(K^2 + n)x^3 - nxy^2] \\ -\alpha_3(x^3 + 3xy^2) - K'xyp_y - \frac{1}{3}n_{sext}(x^3 - 3xy^2)$$

,

$$\alpha_3 \equiv \frac{1}{12}(K'' - 3K^3 - Kn)$$

where the parameter n_{sext} is the field index of the introduced sextupole components.

Note that the compensation problem is greatly simplified for a lattice which is symmetric about the mid-point between absorbers. Taking this symmetry into account, the compensation conditions are reduced to only two equations:

$$< Dn_{sext}u_x^2 >= -<\frac{1}{2}(1 - KD)u_x'^2 + 3[\frac{1}{2}KD(K^2 + n) + \alpha_3 D]u_x^2 - KD'u_x u_x' >$$

$$< Dn_{sext}u_y^2 >=<\frac{1}{2}(1 - KD)u_y'^2 + (3\alpha_3 D - \frac{1}{2}KDn)u_y^2 + K'Du_y u_y' >$$

where the functions u_x and u_y represent the oscillation modes which are antisymmetric about the absorber points of the PIC channel.

To satisfy these two equations, the compensating sextupole field should be designed for the case that $\lambda_x = 2\lambda_y = 4\lambda_0$ by reflecting the field behavior along the beam path by two harmonics as follows:

$$n_{sext} \Rightarrow n_{1sext}\sin k_x s + n_{4sext}\sin 4k_x s$$

As discussed above, the introduction of a strong coupling resonance allows the sextupole design to be simplified by using only one harmonic (lower frequency), instead of two.

B. Compensation for Spherical and Fourth Power Geometrical Aberrations

The spherical and some other geometrical terms to be compensated are seen in the fourth power terms of the expansion of the Hamiltonian:

$$H_4 = \frac{1}{8}(p_x^2 + p_y^2)^2 + \frac{1}{2}(K'xy)^2 - \alpha_3 K(x^4 + 3x^2y^2) - \alpha_4(x^4 - y^4)$$
$$- \beta_4 x^2y^2 - \frac{1}{3}Kn_{sext}(x^4 - 3x^2y^2) - \frac{1}{4}n_{oct}(x^4 + y^4 - 6x^2y^2)$$

Here we have used the following notation:

$$\alpha_4 = \frac{1}{24}(K^2 n - n'' + \delta)$$
$$\beta_4 = -\frac{3}{2}K\alpha_3 + \frac{1}{4}\delta$$
$$\delta = \frac{9}{2}K^4 + K^2 n - 2K'^2 - 3KK'',$$

and n_{oct} is the field index of the introduced octupole components.

The main compensation conditions that are connected to the 4th power of the oscillation mode are antisymmetric about the absorber points of the snake orbit (the symmetric oscillation components damp!). These conditions are:

$$8 < (K\alpha_3 + \alpha_4 + \frac{1}{3}Kn_{sext} + \frac{1}{4}n_{oct})u_x^4 >=< u_x'^4 >$$
$$8 < (\frac{1}{4}n_{oct} - \alpha_4)u_y^4 >=< u_y'^4 >$$
$$4 < (3K\alpha_3 + \beta_4 - Kn_{sext} - \frac{3}{2}n_{oct})(u_x u_y)^2 >=< (u_x' u_y')^2 >$$

The compensating octupole field design for the case that $\lambda_x = 2\lambda_y = 4\lambda_0$ should include a constant component and the two lowest harmonics of the lattice period:

$$n_{oct} = n_{0oct} + n_{1ont}\cos k_0 s + n_{2oct}\cos 2k_0 s .$$

C. Compensation for Higher Order Aberrations

Other 4th power terms result from the second order effect of the 3d power Hamiltonian as shown in the Appendix. Finally, there are several higher power terms in the expansion of the Hamiltonian function which may also require compensation. Compensation for all these terms can be greatly simplified by the use of a coupling resonance, as discussed above. The relevant compensation tools (related multipole field components, beam simulations, and experimental diagnostics) are subject of further study.

IX. TUNE SPREAD DUE TO MUON SPACE CHARGE IN THE PIC CHANNEL

The tune spread due to the space charge of muon bunch under PIC can be estimated from first principles based on:

$$x'' + k^2 x = f_x \qquad (15)$$

$$k^2 \equiv \frac{1}{\beta^2}$$

with space charge transverse force, f_x. The maximum tune shift is produced for particles near the beam center, while for large amplitude particles (beam tails) the shift tends to zero. Therefore, the absolute tune spread value can be found by calculating the tune shift for the center particles. Here, assuming the bunch longitudinal size is large compared to the transverse beam size (round beam), the transverse space charge force can be approximated by linear behavior:

$$f_x \Rightarrow f_0 \equiv \frac{2\pi n_0(s) r_\mu}{\gamma^3 v^2} x,$$

where the density factor $n_0(s)$ is controlled by the beam envelope developed in the PIC process. For a Gaussian charge distribution in the bunch, the density factor is found equal to

$$n_0(s) = \frac{N}{(2\pi)^{3/2}\sigma_\perp^2(s)\sigma_s}$$

with $\sigma_\perp(s)$ and $\sigma_s = const$ the beam rms size in the transverse and longitudinal directions, respectively. Since the tune spread due to space charge is supposed to be small (as for any source of tune spread), the effect can be calculated by a perturbation method. For this, we transform the description of transverse dynamics to variables a and ψ, according to the representation

$$x = a\sin\psi \tag{16}$$

$$x' = ka\cos\psi\,. \tag{17}$$

For unperturbed motion in a focusing lattice, we have $a = const$ and $\psi = ks + const$. Our aim is to calculate the average change of phase advance per betatron period due to the space charge force. For this, we express the phase ψ as a function of x and x' using equations (16) and (17):

$$tg\,\psi = \frac{kx}{x'}.$$

By taking the derivative of this equation along "time" s, we find a relationship

$$\frac{\psi'}{\cos^2\psi} = k - \frac{kxx''}{x'^2};$$

By substituting $\cos\psi$ according to equation (15) and x'' according to equation (17) we find:

$$\psi' = k - \frac{fx}{ka^2}.$$

Now, we will integrate this equation along the unperturbed oscillation trajectory $a = const$, $\psi = ks$, for a particle near the beam center:

$$(\delta\psi')_0 = -\frac{f_0 x}{ka^2} = -\frac{2\pi n_0 r_\mu}{\gamma^3 v^2 k}\frac{x^2}{a^2}$$

or

$$(\delta\psi')_0 = -\frac{Nr_\mu\beta}{\gamma^3 v^2\sqrt{2\pi}\sigma_z}\frac{\sin^2\psi}{\sigma_\perp^2(s)}.$$

In the PIC process, particle trajectories tend to focus at absorber points so that there is a full spread in amplitudes $\Delta a = \sigma_0 \Rightarrow \beta\theta^*$ determined by the angle spread at the absorbers,

$$\theta^{*2} = \frac{3(Z+1)m_e}{2\gamma v^2 m_\mu}. \tag{18}$$

Thus, the beam envelope at the end of the PIC process is described by

$$\sigma_\perp^2(s) \Rightarrow \sigma_0^2 \sin^2 ks + \sigma^{*2},\ \sigma_0^2 >> \sigma^{*2}.$$

Then,

$$-(\delta\psi')_0 \Rightarrow \frac{Nr_\mu\beta}{\gamma^3 v^2 \sigma_z\sqrt{2\pi}} \frac{\sin^2 ks}{\sigma_0^2 \sin^2 ks + \sigma^{*2}} < \frac{Nr_\mu\beta}{\sigma_z\sqrt{2\pi}\gamma^3 v^2 \sigma_0^2}.$$

Note that the contribution from crossing the minimum transverse size (at the absorber) does not dominate the space charge phase advance. In fact, the instantaneous tune shift is almost constant along the beam envelope. Then we find an accurate estimation for phase advance per period of betatron oscillation and tune shift for center particles, and tune spread:

$$(\delta\psi)_0 = \oint (\delta\psi')ds \approx 2\pi\beta(\delta\psi')_0$$

$$\Delta\nu = -\delta\nu_0 \equiv -\frac{(\delta\psi)_0}{2\pi} \approx \frac{Nr_\mu}{\gamma^3 v^2 \sigma_z\sqrt{2\pi}} \frac{\beta^2}{\sigma_0^2} = \frac{Nr_\mu}{\gamma^3 v^2 \theta^{*2} \sigma_z\sqrt{2\pi}}$$

Finally, by taking into account relationship (18), we find:

$$\Delta\nu = \frac{2Nr_e}{3(Z+1)\gamma^2\sigma_z\sqrt{2\pi}}.$$

This formula was used for the numerical estimate of tune spread due to the space charge at PIC equilibrium shown in Table 2.

It should be noted that the tune spread due to space charge is determined in PIC not by the beam transverse phase space (true emittance reduced by PIC), but by the beam characteristic size between absorbers and beam optics along the PIC channel. Remarkably, the tune spread is determined simply by the angle spread at the absorbers, which is not function of beam optics at all. Finally, the resulting expression for tune spread depends only on the absorber atomic number Z. The beam transverse phase space (true emittance) after PIC will be transformed by matching optics to a conventionally defined beam emittance.

X. AN OPTIMIZED PIC DESIGN

In order to approach a practical PIC design, the cooling channel parameters can be modified as the beam is cooled.

First of all and in general, PIC may start with reasonably thick absorbers in order to minimize the beam path while developing the parametric resonance beam envelope.

The maximum initial cooling rate may be limited by the available accelerating RF power. To alleviate this limitation, the initial cooling sections can be effectively isochronous, without RF, where the lattice magnet strengths scale with the decreasing beam momentum. The beam energy could then be restored by RF cavities installed between cooling sections.

Also note that at the beginning and during the middle PIC stages, high precision compensation for aberrations is not required since the beam is not so well focused. Thus the design of the PIC channel for the initial stages can be relatively easy compared to the final stage.

XI. CONCLUSIONS

In this paper we have introduced the basic theory of ionization cooling using parametric resonances and discussed the requirements that must be satisfied to achieve significant beam cooling using this technique. We have derived the effects of chromatic, spherical, and non-linear field aberrations and described how these aberrations can be compensated. That PIC must be accompanied by emittance exchange and that these two techniques are compatible has been demonstrated. We have suggested a particular transport scheme using alternating bends to achieve the two requirements of small dispersion at absorbers and large dispersion where aberrations can be compensated. In addition, the use of a conservative coupling resonance is proposed with the purpose of providing equal parametric resonance cooling rates in the two planes of the beam transport line, and of simplifying the aberration compensation design and control.

Work now underway includes studies of RF schemes to provide regeneration of the energy lost in the absorbers and to use synchrotron motion as an additional correction to chromatic effects [5], wedge engineering limitations, and realistic aberration correction magnets to provide guidance for simulations.

APPENDIX: HAMILTONIAN FRAMEWORK FOR A PLANAR BEAM BEND

Hamilton's method in dynamics provides a convenient and effective analytical technique of formulating, reducing and solving the equation of particle motion in an external field. A particular feature of this method is that it allows one to immediately recognize and utilize the dynamical invariants and canonical relationships between the invariants and some important characteristics of particle motion, such as orbital tunes and dispersions. The method is based on the introduction of the Hamiltonian function of particle coordinates and canonical momenta in a chosen coordinate frame.

In classical dynamics theory, a conventional way of Hamilton's formulation is based on the transformation from Lagrange-Euler equations to Hamilton's equations, either explicitly or through the Hamilton-Jacobi method. Another possibility is to obtain the classical Hamiltonian function and canonical equations starting with the Schrödinger or Klein-Gordon equation of quantum mechanics. In this way, the Hamiltonian formulation appears immediately in classical mechanics as an asymptotic limit of the quantum description; the Lagrange-Euler formulation then is not inquired.

An ordinary Hamilton form is the energy function

$$H_t(\vec{P},\vec{r}) = \sqrt{p^2+m^2} + A_t = \sqrt{(\vec{P}-\vec{A})^2+m^2} + A_t,$$

with equations of motion

$$\frac{d}{dt}\vec{P} = -\frac{\partial}{\partial \vec{r}} H_t; \qquad \frac{d\vec{r}}{dt} = \frac{\partial}{\partial \vec{P}} H_t .$$

A. Hamiltonian function in s-representation of the reference orbit

In the case of a particle beam transported along a curved but planar reference orbit, it is convenient to consider beam path coordinate s as a time argument, while the time can be treated as one of three independent coordinates x, y, t. As usual, we introduce *Frenet frame* with variables x, y, s, t :

$$\vec{r} = \vec{r}_0(s) + x\vec{e}_x + y\vec{e}_y; \quad \vec{r}_0' = \vec{e}_s; \quad \vec{e}_x' = K\vec{e}_s; \quad \vec{e}_s' = -K\vec{e}_x$$

$$Kp_0 = B_0$$

The Hamiltonian function and equations of motion in this representation can be quickly derived using the covariant equation for the wave function $\Psi(\vec{r},t)$, or the relativistic Schrödinger equation

$$[(\hat{P}_t - A_t)^2 - (\vec{P}-\vec{A})^2 - m^2]\Psi(\vec{r},t) = 0 \qquad (19)$$

where $\hat{H}_t \equiv i\hbar\dfrac{\partial}{\partial t}$ and $\hat{\vec{P}} \equiv -i\hbar\dfrac{\partial}{\partial \vec{r}} \equiv \vec{\nabla}$

are the time and space components of the four-vector momentum as a quantum operator. In the Frenet frame the differential operator $\vec{\partial}$ is written as

$$\vec{\nabla} = \vec{e}_x\frac{\partial}{\partial x} + \frac{\vec{e}_s}{1+Kx}\frac{\partial}{\partial s} + \vec{e}_y\frac{\partial}{\partial y}.$$

In the quasi-classical limit, equation (19) can be rewritten, optionally, in two equivalent forms:

A)

$$i\hbar\frac{\partial}{\partial t}\Psi=[\sqrt{(\hat{\vec{P}}-\vec{A})^2+m^2}+A_t]\Psi\equiv\hat{H}_t\Psi \quad ,$$

with corresponding classical equations of motion

$$\frac{d\hat{\vec{P}}}{dt}=-\frac{1}{i\hbar}[\hat{H}_t,\hat{\vec{P}}]\rightarrow\frac{d\vec{P}}{dt}=\{H_t,\vec{P}\}=-\frac{\partial}{\partial\vec{r}}H_t$$

$$\frac{d\vec{r}}{dt}=-\frac{1}{i\hbar}[\hat{H}_t,\vec{r}]\rightarrow\frac{d\vec{r}}{dt}=\{H_t,\vec{r}\}=\frac{\partial}{\partial\vec{P}}H_t$$

where H_t is the conventional form of the Hamiltonian function (*t-representation*):

$$H_t\equiv\sqrt{(\hat{\vec{P}}-\vec{A})^2+m^2}+A_t;$$

Or B)

$$i\hbar\frac{\partial}{\partial s}\Psi=-(1+Kx)[\sqrt{(\hat{H}_t-A_t)^2-(\hat{\vec{P}}_\perp-\vec{A}_\perp)^2-m^2}+A_s]\Psi\Rightarrow H_s\Psi,$$

with equations of motion (in classical limit)

$$P_x'=-\frac{\partial}{\partial x}H_s;\quad x'=\frac{\partial}{\partial P_x}H_s;\quad P_y'=-\frac{\partial}{\partial y}H_s;\quad y'=\frac{\partial}{\partial P_y}H_s$$

$$H_t'=\frac{\partial}{\partial t}H_s;\qquad t'=\frac{\partial}{\partial s}H_s$$

where H_s is the Hamiltonian function in the *s-representation*:

$$\begin{aligned}H_s&\equiv-(1+Kx)[\sqrt{(H_t-A_t)^2-(\vec{P}_\perp-\vec{A}_\perp)^2-m^2}+A_s]\\&=-(1+Kx)(\sqrt{p^2-p_\perp^2}+A_s)\end{aligned}$$

Thus, in the *s*-representation the Hamiltonian coincides with the canonical momentum (with reversed sign)

$$P_s=(1+Kx)(p_s+A_s)$$

taken as a function of energy and transverse momentum according to the covariant equation $E^2-p^2=m^2$:

$$H_s=-(1+Kx)(p_s+A_s)=-(1+Kx)(\sqrt{p^2-\vec{p}_\perp^2}+A_s);$$

$$\vec{p}_\perp=\vec{P}_\perp-\vec{A}_\perp;\qquad p_x=P_x-A_x;\quad p_y=P_y-A_y$$

$$H_t=E+A_t\qquad p^2=E^2-m^2$$

$$H_s=-(1+Kx)[\sqrt{(H_t-A_t)^2-m^2-(P_x-A_x)^2-(P_y-A_y)^2}+A_s] \tag{20}$$

B. Equations for the vector potential of the magnetic field

We use the standard definition of a vector potential of a static magnetic field in vacuum:

$$\vec{B} = \vec{\nabla} \times \vec{A}$$

$$\vec{A} = A_s \vec{e}_s + A_x \vec{e}_x + A_y \vec{e}_y$$

$$\vec{\nabla}^2 \vec{A} = 0; \quad \vec{\nabla}\vec{A} = 0$$

In the Frenet frame we have the following equations:

$$\vec{\nabla}^2 \vec{A} = [\frac{1}{1+Kx}\frac{\partial}{\partial x}(1+Kx)\frac{\partial}{\partial x} + \frac{\partial^2}{\partial y^2} + \frac{1}{1+Kx}\frac{\partial}{\partial s}\frac{1}{1+Kx}\frac{\partial}{\partial s}]\vec{A} = 0$$

and

$$\frac{\partial A_s}{\partial s} + \frac{\partial}{\partial x}(1+Kx)A_x + (1+Kx)\frac{\partial}{\partial y}A_y = 0 .$$

Let us introduce the transverse part of the Laplace operator as

$$\Delta_\perp \equiv \frac{\partial^2}{\partial y^2} + \frac{1}{1+Kx}\frac{\partial}{\partial x}(1+Kx)\frac{\partial}{\partial x};$$

Then, we rewrite equations for vector components , as follows:

$$\Delta_\perp A_s + \frac{1}{(1+Kx)^2}[(1+Kx)\frac{\partial}{\partial s}\frac{1}{1+Kx}(\frac{\partial A_s}{\partial s} + KA_x) + K(\frac{\partial A_x}{\partial s} - KA_s)] = 0$$

$$\Delta_\perp A_x + \frac{1}{(1+Kx)^2}[(1+Kx)\frac{\partial}{\partial s}\frac{1}{1+Kx}(\frac{\partial A_x}{\partial s} - KA_s) - K(\frac{\partial A_s}{\partial s} + KA_x)] = 0$$

$$\Delta_\perp A_y + \frac{1}{1+Kx}\frac{\partial}{\partial s}\frac{1}{1+Kx}\frac{\partial}{\partial s}A_y = 0 .$$

C. Expansion of the s-Hamiltonian

Below we will expand the vector potential and s-Hamiltonian (20) in powers of deviations of particle momentum and transverse coordinates relative to the reference trajectory, in the Frenet frame, including all terms up to the 4th power.

Expansion of the s-Hamiltonian:

$$H_s \approx -(1+Kx)\{p_0 + \Delta p - \frac{p_\perp^2}{2p_0}[1 - \frac{\Delta p}{p_0} + (\frac{\Delta p}{p_0})^2] - \frac{p_\perp^4}{8p_0^3} + A_s\}$$

$$\vec{p}_\perp = \vec{P}_\perp - \vec{A}_\perp$$

Expansion of the vector potential of the magnetic field:

$$A_s \approx A_{s1} + A_{s2} + A_{s3} + A_{s4};$$

$$\vec{A}_\perp \approx \vec{A}_{\perp 1} + \vec{A}_{\perp 2} + \vec{A}_{\perp 3}$$

The first and second order terms of the vector potential:

Longitudinal component:

$$A_{s1} = -B_0(s)x$$

$$A_{s2} = -\frac{1}{2}(\alpha x^2 + ny^2);$$

$$\Delta_\perp (A_{s1} + A_{s2})_0 \Rightarrow 0 \rightarrow \alpha = -n - K^2$$

$$A_{s2} = \frac{1}{2}[(K^2 + n)x^2 - ny^2]$$

Transverse components:

$$\vec{A}_{\perp 1} = 0$$

$$A_{x2} = 0; \qquad A_{y2} = \gamma_{y2} xy$$

$$\gamma_{y2} x - K'x = 0 \rightarrow \gamma_{y2} = K' \rightarrow A_{y2} = K'xy$$

The third order terms of the vector potential

Longitudinal component:

$$\Delta_\perp (A_{s1} + A_{s2} + A_{s3}) = -\frac{\partial^2 A_{s1}}{\partial s^2} + K^2 A_{s1} = (K'' - K^3)x$$

$$(\frac{\partial^2}{\partial x^2} + \frac{\partial^2}{\partial y^2})A_{s3} + K\frac{\partial}{\partial x}A_{s2} - K^2 A_{s1} = (K'' - K^3)x$$

$$A_{s3} = \alpha_{s3}(x^3 - 3xy^2) + \hat{\alpha}_{s3}(x^3 + 3xy^2)$$

$$\hat{\alpha}_{s3} = \frac{1}{12}(K'' - 3K^3 - Kn)$$

Transverse components of the third order:

$$(\frac{\partial^2}{\partial x^2}+\frac{\partial^2}{\partial y^2})A_{x3}=\frac{\partial}{\partial s}KA_{s1}+K\frac{\partial}{\partial s}A_{s1}$$

$$\frac{\partial}{\partial x}A_{x3}+\frac{\partial}{\partial y}A_{y3}+Kx\frac{\partial}{\partial y}A_{y2}+\frac{\partial}{\partial s}A_{s2}=0$$

$$(\frac{\partial^2}{\partial x^2}+\frac{\partial^2}{\partial y^2})A_{y3}+K\frac{\partial}{\partial x}A_{y2}=0$$

$$A_{x3}=\alpha_{x3}(x^3-3xy^2)+\hat{\alpha}_{x3}(x^3+3xy^2)$$

$$A_{y3}=\hat{\beta}_{y3}(y^3+3x^2y)$$

$$\alpha_{x3}=-\frac{1}{3}(KK'+\frac{1}{2}n')$$

$$A_{x3}=-\frac{1}{6}(2KK'+n')(x^3-3xy^2)-\frac{1}{4}KK'(x^3+3xy^2)$$

$$A_{y3}=K'xy-\frac{1}{12}KK'(y^3+3x^2y)$$

The fourth order terms of the vector potential:

longitudinal component only

$$(\frac{\partial^2}{\partial x^2}+\frac{\partial^2}{\partial y^2})A_{s4}=-K\frac{\partial A_{s3}}{\partial x}+K^2x\frac{\partial A_{s2}}{\partial x}-K^3x^2\frac{\partial A_{s1}}{\partial x}-$$

$$-(\frac{\partial^2}{\partial s^2}-K^2)A_{s2}+2Kx(\frac{\partial^2}{\partial s^2}-K^2)A_{s1}+K'x\frac{\partial}{\partial s}A_{s1}$$

$$A_{s4}=\alpha_{s4}(x^4+y^4-6x^2y^2)+\beta_{s4}(x^4-y^4)+\gamma_{s4}x^2y^2$$

$$\gamma_{s4}=-\frac{3}{2}K\hat{\alpha}_{s3}+\frac{1}{4}a$$

$$\beta_{s4}=-\frac{1}{4}K\alpha_{s3}+\frac{1}{24}(K^2n-n'')+\frac{1}{24}a$$

$$a\equiv\frac{9}{2}K^4+K^2n-2K'^2-3KK''$$

Expansion of the s-Hamiltonian using the vector potential:

$$H_1=-(Kp_0-B_0)x-\Delta p\Rightarrow-\Delta p;$$

$$H_2=-Kx\Delta p+\frac{P_\perp^2}{2p_0}-KxA_{s1}-A_{s2}$$

$$H_3 = \frac{P_\perp^2}{2p_0}(Kx - \frac{\Delta p}{p_0}) - KxA_{s2} - A_{s3} - \frac{\vec{P}_\perp \vec{A}_{\perp 2}}{p_0}$$

$$H_4 = -Kx(\frac{\vec{P}_\perp \vec{A}_{\perp 2}}{p_0} + \frac{P_\perp^2}{2p_0^2}\Delta p + A_{s3}) + \frac{\vec{A}_{\perp 2}^2}{2p_0} + \frac{P_\perp^4}{8p_0^3} - \frac{\vec{P}_\perp \vec{A}_{\perp 3}}{p_0} + \frac{P_\perp^2 (\Delta p)^2}{2p_0^3} - A_{s4}$$

D. Second order Hamiltonian function for the linear optic design

$$H_2 = -Kx\Delta p + \frac{P_x^2 + P_y^2}{2} + \frac{1}{2}[(K^2 - n)x^2 + ny^2]$$

Linear equations:

$$x'' + (K^2 - n)x = K\Delta p; \quad y'' + ny = 0$$

$$x = D\frac{\Delta p}{p} + x_b; \qquad D'' + (K^2 - n)D = K$$

$$K(s) = K(s + \lambda_0); \qquad n(s) = n(s + \lambda_0).$$

E. The third power Hamiltonian

Combining all the 3d power terms of the above expansions of the Hamiltonian and vector potential, we obtain the 3d power Hamiltonian part as follows:

$$H_3 = -\frac{1}{2}(p_x^2 + p_y^2)(q - Kx) - \frac{1}{2}K[(K^2 + n)x^3 - nxy^2]$$
$$-\alpha_3(x^3 + 3xy^2) - K'xyp_y - \frac{1}{3}n_{sext}(x^3 - 3xy^2)$$
$$\alpha_3 \equiv \frac{1}{12}(K'' - 3K^3 - Kn)$$

where the parameter n_{sext} is the field index of the introduced sextupole components.

F. The fourth power terms

Combining all the 4th power terms of the above expansions of the Hamiltonian and vector potential, we obtain the 4th power Hamiltonian part as follows:

$$H_4 = \frac{1}{8}(p_x^2 + p_y^2)^2 + \frac{1}{2}(K'xy)^2 - \alpha_3 K(x^4 + 3x^2y^2) - \alpha_4(x^4 - y^4)$$
$$-\beta_4 x^2y^2 - \frac{1}{3}Kn_{sext}(x^4 - 3x^2y^2) - \frac{1}{4}n_{oct}(x^4 + y^4 - 6x^2y^2)$$

Here we use the following notation:

$$\alpha_4 = \frac{1}{24}(K^2 n - n'' + \delta)$$

$$\beta_4 = -\frac{3}{2}K\alpha_3 + \frac{1}{4}\delta$$

$$\delta = \frac{9}{2}K^4 + K^2 n - 2K'^2 - 3KK'',$$

and n_{oct} is the field index of the introduced octupole components.

More terms of the 4th power on transverse variables arrive as secondary effects from the 3d order Hamiltonian. They are generally formulated as resulting from a Poisson bracket as follows:

$$H_4^{(3)} = \frac{1}{2}\{H_3, \hat{H}_3\}$$

where

$$\hat{H}_3 \equiv \int H_3(s)ds,$$

with the Hamiltonian term H_3 considered as a function of time *s* with constant particle trajectory parameters *a* and *b*.

REFERENCES

[1] Y. Derbenev and R. P. Johnson (Phys. Rev. Special Topics Accel. and Beams 8, 041002 (2005)) http://www.muonsinc.com/reports/PRSTAB-HCCtheory.pdf

[2] L. D. Landau and E. M. Lifshits, Theoretical Physics v. 8, Electrodynamics of continuous media 1960 QC 518.L23.

[3] Y. Derbenev and R. P. Johnson, op. cit.

[4] R.P.Johnson,C.M.Ankenbrandt, C. Bhat, M. Popovic, S.A.Bogacz, Y. Derbenev, "Muon Bunch Coalescing" Proceedings of PAC07, Albuquerque, NM, http://pac07.org/proceedings/PAPERS/THPMN095.PDF

[5] K. Beard et al., SIMULATIONS OF PARAMETRIC RESONANCE IONIZATION COOLING OF MUON BEAMS, http://accelconf.web.cern.ch/AccelConf/p05/PAPERS/TPPP013.PDF

SIMULATIONS OF PARAMETRIC RESONANCE IONIZATION COOLING OF MUON BEAMS *

Kevin Beard#, S. Alex Bogacz, Yaroslav Derbenev (Jefferson Lab, Newport News, Virginia),
Katsuya Yonehara (Illinois Institute of Technology, Chicago, Illinois),
Rolland P. Johnson, Kevin Paul, Thomas J. Roberts (Muons, Inc, Batavia)

Abstract

Parametric-resonance ionization cooling (PIC) is being developed to create small beams so that high muon collider luminosity can be achieved with fewer muons. In the linear channel that is studied in this effort, a half integer resonance is induced such that the normal elliptical motion of particles in $x-x'$ phase space becomes hyperbolic, with particles moving to smaller x and larger x' as they pass down the channel. Thin absorbers placed at the focal points of the channel then cool the angular divergence of the beam by the usual ionization cooling mechanism where each absorber is followed by RF cavities. Thus the phase space of the beam is compressed in transverse position by the dynamics of the resonance and its angular divergence is compressed by the ionization cooling mechanism. We report the first results of simulations of this process, a study of the compensation of chromatic aberration by using synchrotron oscillations.

INTRODUCTION

The concepts and basic equations for PIC are described in another paper submitted to this conference [1]. The essential practical question for PIC is how well detuning effects can be compensated. Chromatic aberration, the detuning effect we consider here, is where the momentum-dependent betatron frequency causes off- momentum particles to be out of resonance with the focusing lattice. Recent analytic studies [2] show that by choosing suitable synchrotron motion parameters, the resonance condition can be maintained. This paper reports the first simulation to test this prediction using the OptiM program [3].

SOLENOID TRIPLET CELL

Our studies of optimum lattice configurations indicate that an excellent cell for PIC consists of an alternating solenoid triplet. This provides strong focusing, so that the horizontal and vertical betatron phases advance by 3π across the cell and by π between the absorbers (indicated by markers). This configuration provides a periodic half-integer and integer resonant lattice.

The total length of the p = 286.8 MeV/c cell is 7.2 m with the Initial betas of 21 cm. In the transfer matrix formalism of OptiM the three "soft edge" solenoids have fields of B_0= -34.1, 32.4, and -34.1 kG with lengths L=80, 130, and 80 cm, respectively, and radius a=20 cm. The Larmor wave number is $k = eB_0/Pc$.

The periodic solution of the cell is illustrated in terms of Twiss functions below:

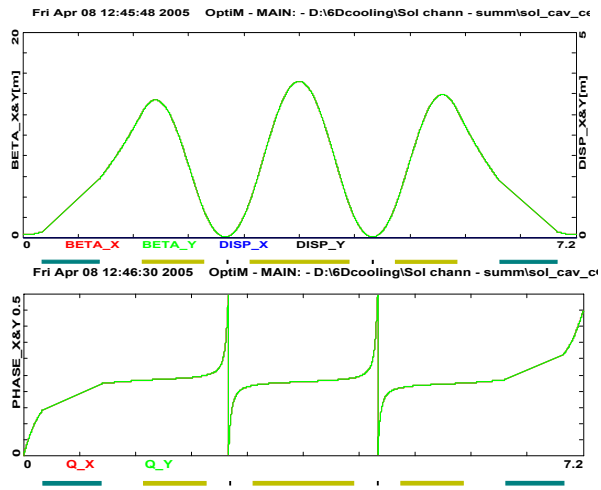

Figure 1: Beta functions and phases for the solenoid triplet cell. Thin absorbers are placed at the two central focal points. In the simulations for Fig. 2 the lost energy is simply replaced at the absorbers. For Fig. 3, 400 MHz RF cavities shown as blue bars replace the lost energy and provide synchrotron motion.

'Soft edge" Solenoid – matrix implementation

If the aperture is equal to zero a solenoid is considered as an ideal linear solenoid with transfer matrix equal to

$$\mathbf{M}_{sol} = \begin{bmatrix} \frac{1+\cos(kL)}{2} & \frac{\sin(kL)}{k} & \frac{\sin(kL)}{2} & \frac{1-\cos(kL)}{k} \\ -\frac{k\sin(kL)}{4} & \frac{1+\cos(kL)}{2} & -k\frac{1-\cos(kL)}{4} & \frac{\sin(kL)}{2} \\ -\frac{\sin(kL)}{2} & -\frac{1-\cos(kL)}{k} & \frac{1+\cos(kL)}{2} & \frac{\sin(kL)}{k} \\ k\frac{1-\cos(kL)}{4} & -\frac{\sin(kL)}{2} & -\frac{k\sin(kL)}{4} & \frac{1+\cos(kL)}{2} \end{bmatrix}.$$

If the aperture is non-zero there is a correction related to the finite length of the solenoid edge. This correction decreases the solenoid total focusing in comparison with the ideal solenoid of the same length. In this case the solenoid length is determined by:

$$L = \frac{1}{B_0}\int_{-\infty}^{\infty} B_z(s)\,ds.$$

* Supported in part by DOE SBIR grants DE-FG02-03ER83722, and 04ER84016.
# Beard@JLab.org

The correction to the edge focusing at each solenoid edge is determined by the following formula:

$$\Phi_{edge} = \frac{1}{2}\left(\int_{-\infty}^{\infty} B_z^2(s)\, ds - B_0^2 L \right) = -\frac{k^2 a}{8} .$$

Therefore, the edge focusing of a solenoid can be described by an axially symmetric multipole (m = –1) through the following transfer matrix:

$$\mathbf{M}_{edge} = \begin{bmatrix} 1 & 0 & 0 & 0 \\ -\Phi_{edge} & 1 & 0 & 0 \\ 0 & 0 & 1 & 0 \\ 0 & 0 & -\Phi_{edge} & 1 \end{bmatrix},$$

$$\Phi_{edge} = -\frac{k^2 a}{8}$$

The final transfer matrix describing a 'soft edge' solenoid can be expressed as:

$$\mathbf{M}_{soft\,sol} = \mathbf{M}_{edge}\, \mathbf{M}_{sol}\, \mathbf{M}_{edge} .$$

THIN ABSORBER AND RF

Ionization cooling due to energy loss (-Δp) in a thin absorber followed by immediate re-acceleration (Δp) can be described as:

$$\Delta\theta_{\perp} = -\theta_{\perp}\frac{\Delta p}{p}$$

The corresponding canonical transfer matrix can be written as

$$M_{abs} = K \begin{bmatrix} 1 & 0 & 0 & 0 \\ 0 & 1-\frac{\Delta p}{p} & 0 & 0 \\ 0 & 0 & 1 & 0 \\ 0 & 0 & 0 & 1-\frac{\Delta p}{p} \end{bmatrix} K^{-1}$$

$$K = \begin{bmatrix} 1 & 0 & 0 & 0 \\ 0 & 1 & -k/2 & 0 \\ 0 & 0 & 1 & 0 \\ k/2 & 0 & 0 & 1 \end{bmatrix} \quad \hat{\mathbf{x}} \equiv \begin{bmatrix} x \\ p_x \\ y \\ p_y \end{bmatrix} \quad \mathbf{x} \equiv \begin{bmatrix} x \\ \theta_x \\ y \\ \theta_y \end{bmatrix}$$

where $k = eB_z / pc$ and $\hat{\mathbf{x}} = K\mathbf{x}$.

normalized emittance: $\varepsilon_x/\varepsilon_y$	mm	30
longitudinal emittance: ε_l ($\varepsilon_l = \sigma_{\Delta p}\,\sigma_z/m_\mu c$)	mm	0.8
momentum spread: $\sigma_{\Delta p/p}$		0.01
bunch length: σ_z	mm	30
momentum	MeV/c	286.8

Table 1: Initial parameters for simulation studies.

In the simulation Δp/p of 0.05 was used to mock-up the effect of a thin (4 cm) Be plate followed by re-acceleration (Δp = 14 MeV/c).

To induce synchrotron oscillation into the channel dynamics two 400 MHz RF cavities at zero crossing are added symmetrically to each cell. The cavity gradient of 17.3 MeV/m was chosen to provide appropriate height of a stationary bucket with a synchrotron phase advance of about 2π/8 per cell. Since the RF cavities in the simulation provide some focusing, it was necessary to reset the triplet solenoid values to reestablish the resonant condition (B=-33.9, 32.1, -33.9).

SIMULATIONS

The simulation involves tracking 5000 particles defined by a 6D Gaussian with the parameters from the Table through a PIC channel consisting of 8 periodic cells (two absorbers per cell), or one synchrotron oscillation period. A sequence of transverse (*x, x'*) and longitudinal (ş, dp/p × 1000) phase space 'snapshots' starting with the initial distribution and followed by the 'snapshots' taken after passing through two cells is collected is shown in Figs 2 and 4. In Fig. 2 the beam energy lost in the absorber is simply replaced as described in the previous section. In the simulations shown in Fig. 4, RF cavities are used to generate synchrotron motion as well as to replace the energy lost in the absorber.

CONCLUSIONS

Comparing Fig. 3 with Fig. 2 of the betatron and synchrotron phase space evolution through 8 solenoid triplet cells, it is easy to see that the synchrotron motion makes a significant difference. In Fig. 2 the tails of the betatron distribution are larger and particles are lost. In Figs 3 and 4, the final $x - x'$ plot shows the promise of PIC: the x distribution has narrowed from the initial one, and the x' distribution shows the effects of ionization cooling. However, the evaluation of the actual cooling of the beam awaits a proper simulation using all the power of the most realistic codes.

The simulation model used here has provided a first confirmation that our understanding of PIC is correct and that compensation for chromatic aberrations can be made as suggested. We will soon test the theory that angular aberrations can be compensated as well and include multiple scattering and energy straggling effects using G4Beamline [4].

REFERENCES

[1] Yaroslav Derbenev and Rolland P. Johnson, Ionization Cooling Using a Parametric Resonance, this conference.
[2]Y. Derbenev and R. P. Johnson, Phys. Rev. ST Accel. Beams **8,** 041002 (2005).
[3] V. Lebedev, http://www-bdnew.fnal.gov/pbar/organizationalchart/lebedev/OptiM/optim.htm
[4] T.Roberts, http://www.muonsinc.com/g4beamline.html

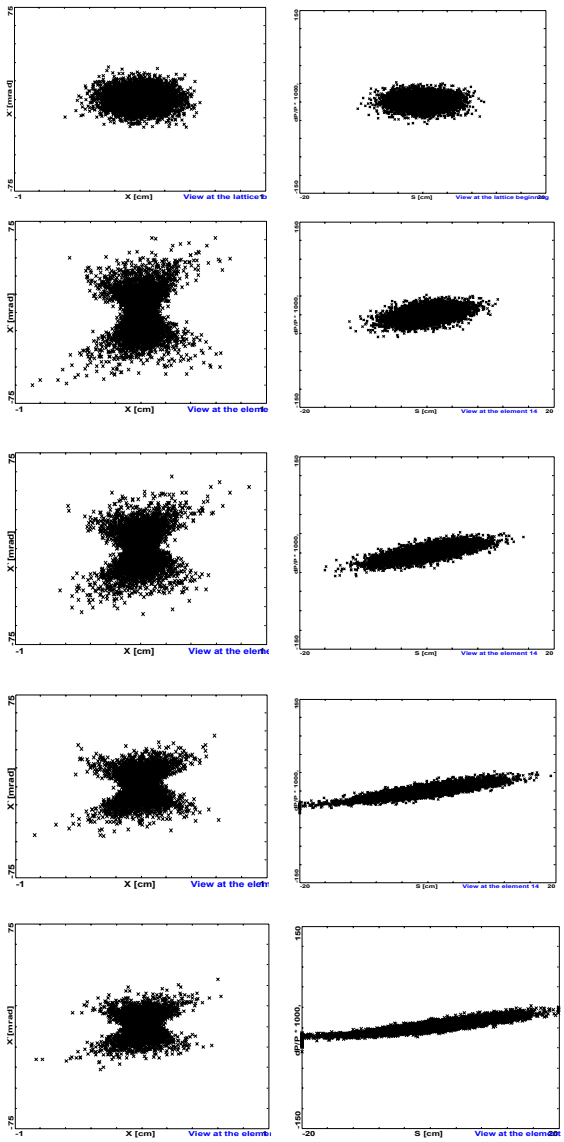

Figure 2: PIC simulation "snapshots" of $x-x'$ (LEFT) and $s-\Delta p/p$ (RIGHT) phase space without synchrotron motion to correct chromatic aberration. Reading from top to bottom, each snapshot corresponds to passage through two of the cells shown in Fig. 1.

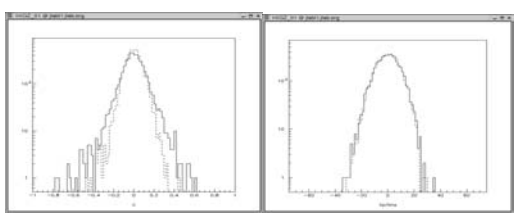

Figure 3: The left histogram displays the final x distribution in cm with a solid line for the case without, and a dotted line for the case with, synchrotron RF. The right histogram displays the x' distribution in milliradians for the two cases.

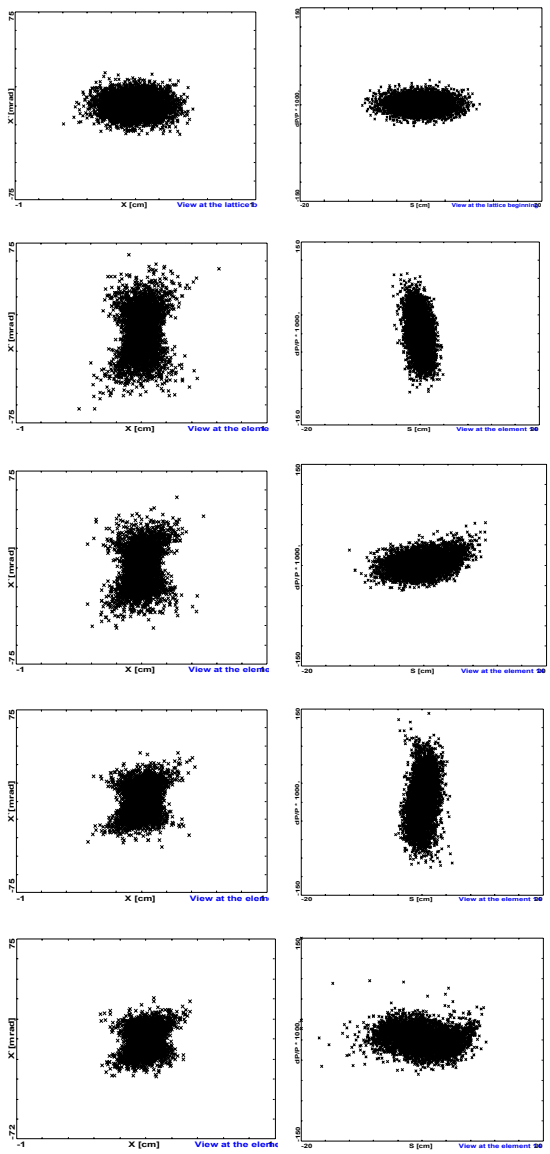

Figure 4: PIC simulation "snapshots" of $x-x'$ (LEFT) and $s-\Delta p/p$ (RIGHT) phase space with synchrotron motion compensation of chromatic aberration. The transverse phase space with synchrotron motion is seen to be smaller than in Fig. 2. The RF bunch rotation of one synchrotron period is seen on the RIGHT plots. The growth of the longitudinal emittance is consistent with the conclusion that emittance exchange and longitudinal cooling will have to be combined with PIC.

SIMULATIONS OF PARAMETRIC-RESONANCE IONIZATION COOLING*

David Newsham#, Rolland P. Johnson, Richard Sah, Muons, Inc., Batavia, IL.
S. Alex Bogacz, Yu-Chiu Chao, Yaroslav Derbenev, Jefferson Lab, Newport News, VA.

Abstract

Parametric-resonance ionization cooling (PIC) is a muon-cooling technique that is useful for low-emittance muon colliders. This method requires a well-tuned focusing channel that is free of chromatic and spherical aberrations. In order to be of practical use in a muon collider, it also necessary that the focusing channel be as short as possible to minimize muon loss due to decay. G4Beamline numerical simulations are presented of a compact PIC focusing channel in which spherical aberrations are minimized by using design symmetry.

INTRODUCTION

PIC [1] takes advantage of an induced half-integer resonance in a ring or beam line where the normal elliptical motion of the particles in $x - x'$ phase space becomes hyperbolic. Thin absorbers placed at the focal points of the channel will then cool the angular divergence of the beam by the usual ionization cooling mechanism. The purpose of the resonance is to cause the particles to move to smaller x and larger x' at the absorber plates as they travel longitudinally down the lattice. (This is almost identical to the technique used for half-integer extraction from a synchrotron where the hyperbolic trajectories go to small x' and larger x to pass the wires of an extraction septum.) With the absorbers properly designed based on the dispersive characteristics of the beamline, the longitudinal emittance can be maintained by emittance exchange, while the transverse emittance is reduced. RF cavities will be used for energy recovery, either after each absorber, or after a series of cells.

The basic theory of PIC is being developed to include aberrations and higher order effects, and an understanding of the basic optical features of an appropriate beamline is required prior to implementing aberration control. Both OPTIM [2] and G4beamline (G4BL) [3] were used to simulate linear channels of alternating dipoles, quadrupoles, and solenoids with a schematic layout shown in Figure 1. Understanding of the non-linear and resonant dynamics will only come from a clear understanding of the linear dynamics of the lattice.

OPTIM SIMULATIONS

Initially, OPTIM [2] was used to simulate the beamline to determine a basic design and set of starting parameters.

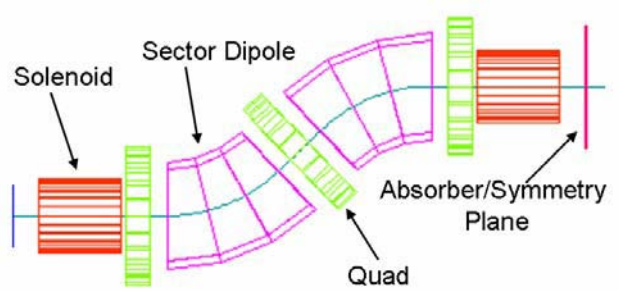

Figure 1:..One cell of the G4BL implementation of a PIC lattice.

Since OPTIM is a linear, transverse matrix model, it is not well suited to understand the lattice beyond the parameter space where each of the elements is linear, compact and non-interacting. Two tracks for the initial simulations were taken. The first used solenoid and quadrupole field values that gave betatron oscillations away from any resonances (including the half-integer resonance). The transverse beta-functions and dispersion are shown in Figure 2. The other line of study focused on field values that tuned the lattice to near the half-integer resonance.

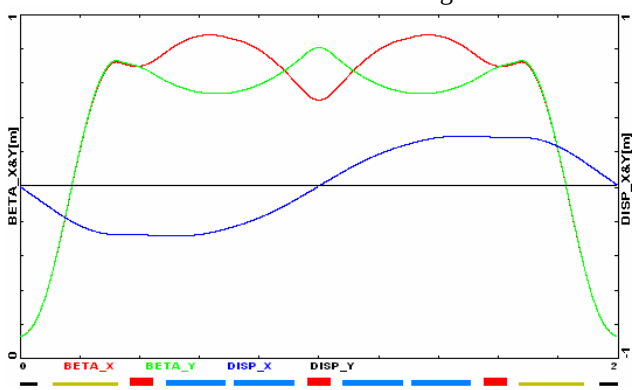

Figure 2: OPTIM simulation result for a single 2 m long "detuned" PIC Cell. The red and green lines are the x and y beta functions, and the blue line is the dispersion in the x direction. The dispersion in the y direction has a value of zero at all positions along the reference orbit.

G4BEAMLINE SIMULATIONS

Initial studies in G4BL were performed on the detuned lattice as designed with OPTIM. The automatic dipole tuning in G4BL greatly simplified the process of finding the periodic reference particle orbit. Figure 3 shows the results of a G4BL simulation of the "detuned" lattice based on the OPTIM design. The G4BL lattice had dramatically different values for the solenoid and quadrupole fields. These differences are partially because

*Work supported by DOE SBIR grant DE-FG02-04ER84016.
#newsh@muonsinc.com

G4BL does not yet include end fields on either the sector dipole magnets or on the "generic multipole" magnets that were used to create the quads. Despite the differences in the detailed field values of the beamline elements, the general appearance of the G4BL results look remarkably similar in shape and relative amplitude to the results from the OPTIM simulation.

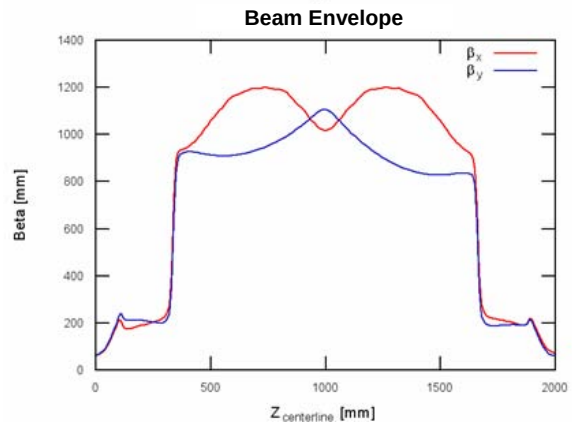

Figure 3: Transverse beam envelopes (expressed as beta functions) of the "detuned" PIC cell as calculated from G4BL simulations.

Solenoid Fields

Initial simulations of the snake lattice lead to two fundamental issues resulting from the solenoid magnets. The use of solenoidal focusing intimately coupled the two transverse directions and the implementation of the solenoids in G4BL lead to long end fields if a coil of any acceptable aperture was used. The coupling problem was removed by using two identical bucked solenoids in a "counterwound" configuration. Basically, the second solenoid reverses any mixing in the first solenoid.

The initial simulations used the "solenoid" element in G4BL that constructs a field map based on adding the field values from many infinitely thin current sheets. This results in a simple to implement magnet that satisfies Maxwell's Equations. Unfortunately, the long end fields also interfere with the vertical dipole fields causing a kick in the particle motion that lead to rapid (within a few cells) ejection from the lattice. In order to better understand the effect of each element, the solenoid was replaced with a field map (see Figure 4) with no radial dependence of the axial field and an extremely short fringe field. While this field profile still satisfied Maxwell's Equations to first order in radius, it was extremely non-physical in the sense that it would be extremely difficult, if not impossible to construct. Since the point of this initial study was to determine the linear lattice and then proceed to investigate aberration control, the idealized solenoid field was not seen as an important issue at this point.

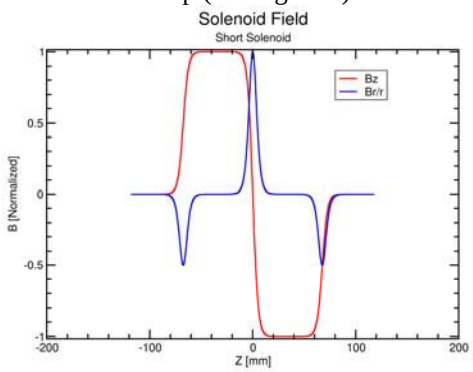

Figure 4: Field map of the "short" solenoid magnet.

Monochromatic Transverse Motion

The modification to the solenoid magnet model increased the allowable size of the magnet, resulting in the ability to model more realistic beam sizes (at the expense of unrealistic magnets). Figure 5 shows the transport line for a "detuned" structure for transverse emittances near the anticipated value. The introduction of absorbers was not performed at this stage because without longitudinal studies, no real understanding of the cooling will be achieved. These cells were tuned to transmit a 1 mm mrad beam while maintaining the spot size, but are displayed with a 200 mm mrad beam. In addition to demonstrating the stability of the lattice, Figure 5 also shows the two anticipated layouts. The "snake" lattice meanders with each cell being a translated version of the previous cell. The "chicane" lattice is named because it appears similar to a beamline chicane, although its purpose is different. These design layouts each have different features, but at the basic level, they are the same. The major differences arise based on the symmetry of the cell layout.

Figure 5: G4BL simulation of a large, monochromatic beam in both the "snake" and "chicane" design layouts (solenoid fields are present as shown in Figure 1, but invisible).

Dispersion Effects

The first place dispersion and the derivative of dispersion (dispersion prime) must be considered is with the inclusion of a momentum spread. An examination of the cell entrance and exit in Figure 2 shows that while there is no dispersion at these symmetry points, there is a definite slope in the dispersion curve. In practice, an entrance/exit cell must be designed to match this lattice to the dispersion-free beamline. In terms of simulations, the input beam must be constructed so that it is matched to this dispersive behavior.

Figure 6 shows the simulation results of 100 particles, all starting with $x = y = x' = y' = 0$ and a momentum spread of ±5%. For this detuned betatron advance, the snake lattice appears more unstable to a mismatch in the dispersion prime as compared to the chicane lattice. As additional cells were added, the loss of particles in the snake lattice disappeared while losses in the chicane lattice began to grow significantly. Although not shown, when the initial value of x' matched the value at the edges of the lattice cell, the snake lattice showed significantly improved performance. Detailed studies of the chicane lattice have yet to be performed using G4BL.

Figure 6: G4BL simulation of the snake and chicane layouts with unmatched dispersion prime.

SNAKE VS CHICANE LAYOUT

The difference between a snake layout and a chicane layout only appears after the first cell, before then, the two layouts are identical. While this might appear an obvious statement, it is critical to understanding the differences in behavior. The nature of the chicane layout is that of a 2-cell structure, thus, it will have dispersion solutions that are different than the periodic solution in Figure 2. In addition, for the same values of the lattice elements, there are several possible dispersion solutions as more cells are added. Because of a difference in symmetry, one feature of the chicane layout is that the geometric spherical aberration should be mitigated. This aberration will unavoidably arise from the use of dipole magnets, but in a beamline with total reflection symmetry, an exact cancellation can occur. The chicane layout displays this symmetry, while the snake does not.

Figure 7 shows the results of an OPTIM simulation to test this feature. The initial beam (a) is an OPTIM-determined matched beam with a transverse emittance of 100 mm mrad and almost no momentum spread. (b) and (c) show the output from pushing the initial beam through two cells of a snake and chicane (respectively) layout beamline. The output from the snake channel (b) shows a slight bulge on the positive *x* side and several particles straggling out to much larger *x* values. The most notable change is in the *x* phase space where the particles with large *x*-momentum appear to be primarily responsible for the position excursion. This is expected since the aberration is dipole dependent and the bend is only in the *x*-plane. Additionally, the *y*-phase space shows no appreciable change as would be expected with all of the dispersive elements only in the *x*-direction.

The chicane design, however, appears to have significantly canceled the effect of this spherical aberration. While notable deviations between the input and output beams exist in the chicane layout, these would be expected since the effect must be added in the first cell (since it is identical to the first cell of the snake layout), then subtracted in the second cell, the overall affect on the beam profile is significantly reduced.

Figure 7: OPTIM simulation of a matched muon beam through both a snake and a chicane layout of identical lattices. a) Input beam b) output from snake layout and c) output from chicane layout.

TRANSVERSE PHASE SPACE

Initial investigations into the transverse phase space mapping of this lattice indicate strange behavior. Preliminary analysis shows apparent unstable fixed points at positive and negative values of *x'* and $x = 0$. The phase space map in the *y*-phase space shows identical behavior. This behavior is currently under continued study.

SUMMARY

Simulations of the PIC lattice in both G4Beamline and OPTIM are progressing. Much of the linear optics of the snake layout have been investigated and are expected to apply directly to the chicane layout. The inclusion of the dispersive effects in the initial longitudinal profile are an important first step in understanding the full 6D motion of these lattices and their ultimate ability to realize the needed cooling factors. Strange transverse phase space behavior requires additional study to if aberration control is to succeed.

REFERENCES

[1] Yaroslav Derbenev et al., COOL05.
[2] OPTIM, http://www-bdnew.fnal.gov/pbar/organizationalchart/lebedev/OptiM/optim.htm
[3] G4beamline, http://g4beamline.muonsinc.com

OPTICS FOR PHASE IONIZATION COOLING OF MUON BEAMS*

Y. Derbenev, S. A. Bogacz, Jefferson Lab, Newport News, VA, USA
R. P. Johnson#, Muons, Inc., Batavia, IL, USA

Abstract

The realization of a muon collider requires a reduction of the 6D normalized emittance of an initially generated muon beam by a factor of more than 10^6. Analytical and simulation studies of 6D muon beam ionization cooling in a helical channel filled with pressurized gas or liquid hydrogen absorber indicate that a factor of 10^6 is possible. Further reduction of the normalized 4D transverse emittance by an additional two orders of magnitude is envisioned using Parametric-resonance or Phase Ionization Cooling (PIC). To realize the phase shrinkage effect in the parametric resonance method, one needs to design a focusing channel free of chromatic and spherical aberrations. We report results of our study of a concept of an aberration-free wiggler transport line with an alternating dispersion function. Resonant beam focusing at thin beryllium wedge absorber plates positioned near zero dispersion points then provides the predicted PIC effect.

INTRODUCTION

Muon collider luminosity depends on the number of muons in the storage ring and on the transverse size of the beams in collision. Ionization cooling (IC) as it is presently envisioned [1] will not cool transverse beam sizes sufficiently well to provide adequate luminosity without large muon intensities. A new idea to combine ½ -integer parametric resonances and IC (PIC) [2] in a linear focusing channel has been proposed that will lead to much smaller transverse beam emittances so that high luminosity in a muon collider can be achieved with fewer muons. In this report we describe basic principles and potentials of PIC and address the main constraints associated with tune spreads and energy straggling in the muon beam.

OVERVIEW OF A PIC CHANNEL

PIC takes place in the sections of a cooling channel where the beam is strongly focused onto beryllium wedges and where a special dispersion function is used to create the conditions for aberration correction and emittance exchange (EMEX). Since the dispersion oscillates in these sections, we call them snake phase cooling (SPC) sections. A basic constraint of the PIC channel is that there must be regular replenishment by RF cavities of the energy lost in the beryllium wedge absorbers. Since the beam must pass through several cavity apertures, the focusing must be relatively weak in each RF section. So there must be a compressor transition section between each strong focusing SPC section and the next RF section and an expander transition section between each RF section and the next SPC section. Another feature is a skew quad section to exchange the x and y planes since we have in mind that the whole channel will have only horizontal bends in the PIC region where a very special dispersion function is required. For optimal EMEX, the three cooling decrements should be equal on average along the cooling channel; this requires a relationship between dispersion D and the absorber wedge height h [3]:

$$(D/h) = 2 - (4\beta^2/3) \qquad (1)$$

To take advantage of the magnet apertures, the maximum beam size should be more or less constant. That is, as the beam cools, the focusing should increase. The maximum beta should increase and the minimum should decrease until it approaches the thickness of the absorber plate. This process is described by the usual relationships: $\sigma_{\max} \approx \sigma_0$; $\sigma_{\max} \cdot \sigma_{abs} = f\varepsilon$; $\beta_{\max}\beta_{abs} = f^2$; $\beta_{abs} \geq w$; and $\beta_{abs} \Rightarrow w_{final}$.

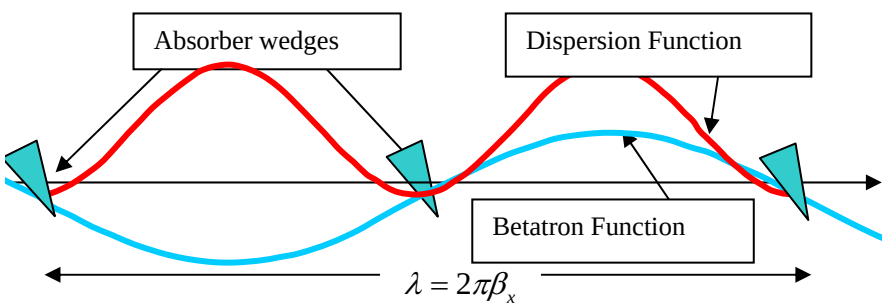

Figure 1: Schematic of a snake phase cooling (SPC) section, where wedge absorbers are placed at symmetric locations relative to the dispersion function, which has a period half that of the betatron function. Chromatic aberration correction sextupoles are placed at the maxima of the dispersion functions. The wedge absorbers require smaller dispersion for EMEX to control the momentum spread during the cooling process.

*Supported by U.S. DOE Contract No. DE-AC05-84ER40150 and SBIR grant DE-FG02-04ER84016
rol@muonsinc.com

Here ε_0 and σ_0 are, respectively, the initial beam emittance and size (after 6D cooling) in a channel with characteristic focal parameter *f*. $\sigma_{\max}$ and $\beta_{\max}$ are the beam size and beta function at the entrance to a SPC section, while β_{abs} and σ_{abs} are the beta function and beam size at the absorber plates of the SPC. These last two parameters together with the beam emittance progressively decrease cell by cell of the cooling channel, while $\beta_{\max}$ (i.e. beam expansion after RF to next SPC) is designed correspondently to grow. The minimal β_{abs} is limited by the plate thickness w, which (together with achievable emittance and cooling channel length), in turn, is limited by beam loss due to muon decay (and also by the tuning demands). With this design concept, we avoid a large increase of beam size at the entrance to the SPC compared to its characteristic magnitude after the 6D cooling, while achieving a maximally strong beam focus at the absorber plates at the end of cooling channel. For optimum beam extension:

$$(\beta_{\max} / f) = (\varepsilon_0 / \varepsilon) \Rightarrow (f / w_{final})$$

BASIC BEAM TRANSPORT AND LINEAR OPTICS DESIGN PRINCIPLES

The main constraint of the parametric resonance ionization cooling design is to combine low orbit dispersion at the wedge absorber plates with the necessary large dispersion in the space between plates required to compensate for chromatic aberration. These conflicting requirements can be resolved in a channel with plane wiggling beam orbit created by an alternating dipole field (see Figure 1).

In such a channel, the dispersion alternates along with the wiggling orbit. The absorber plates then are positioned near zero dispersion points. Obviously, the betatron (i.e. focusing) wave length must not be same as the bend and dispersion period, but it can be two or four times longer then that. Figure 2 shows an example of such a cooling channel lattice cell with additional components to provide space for RF to replenish the energy lost in the absorbers.

TUNING DEMANDS

Strong focusing of the muon beam at the absorber plates (especially in the final cells) requires a sufficiently small spread of the focal parameter *f* caused by various aberrations (chromatic, spherical, third order non-linear fields, and space charge detuning). The general requirement for this condition is

$$\Delta f \cdot \pi q << \beta_a \approx f \cdot (\varepsilon / \varepsilon_0) \Rightarrow w_{final}.$$

Here *q* is the number of absorber plates in a cell (which may vary from a maximum at start to a minimum in th final cell). The first three aberrations can be compensated by sextupoles and octupoles. Detuning due to space charge cannot be compensated.

Calculation of the space charge defocusing impact on phase ionization cooling leads to the relation

$$\frac{\Delta f}{f} = \frac{f}{\sigma_z \sqrt{2\pi}} \frac{N r_\mu}{\beta \gamma^2 \varepsilon_0}.$$

Here *N* is the number of muons in a bunch, σ_z is the rms bunch length, and r_μ is the classical radius of the muon. This relation shows that that the space charge detuning in the SPC cells is determined by the initial beam emittance ε_0 and not the cooled emittance ε.

Table I shows the expected PIC performance for a muon collider cooling channel.

Table I: Potential PIC effect

Parameter	*Unit*	*Initial*	*Final*
Beam momentum, p (average)	MeV/c	100	100
Distance between plates, $\lambda/2$	cm	40	40
Plate thickness, w	mm	6.4	1.6
Intrinsic energy loss rate (Be), $E_{\mathrm{int}\,r}$	MeV/m	600	600
Average energy loss in cooling section	MeV/m	20	5
Transverse emittance, norm.	μm	600	25
Beam transverse size at plates	mm	6.0	0.15
Angle spread at plates, $\theta_x = \theta_y$	mrad	200	200
PIC channel length	m	150	
Integrated energy loss	GeV	0.7	
Beam loss due to muon decay	%	20	
Number of particles/bunch		10^{11}	
Space charge tune spread, $\Delta f / f$		10^{-3}	

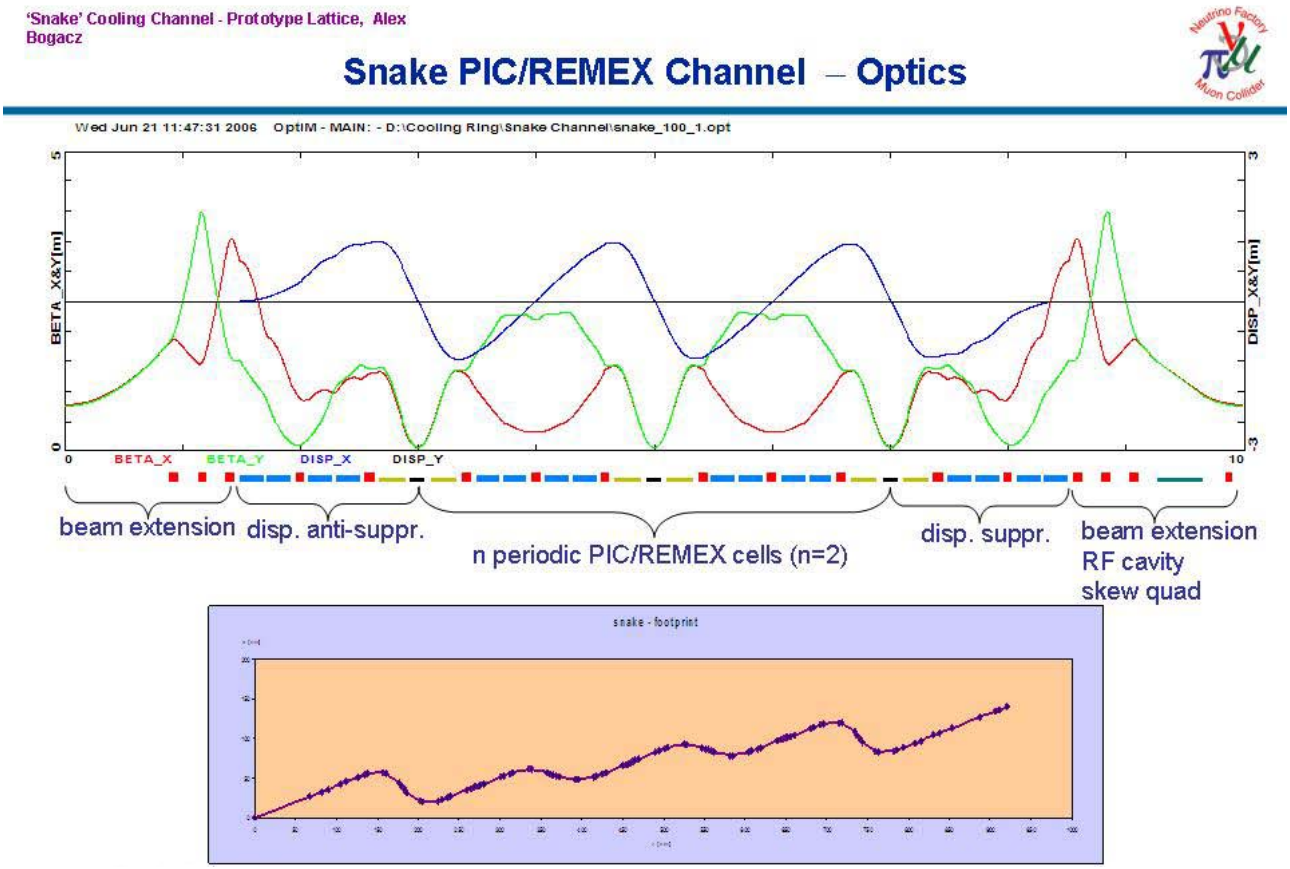

Figure 2: OptiM displays of a PIC (or REMEX) cooling lattice cell. The upper graph has the lattice functions for a 10 m long cell with sequential sections for beam extension, dispersion creation, SPC, dispersion suppression, beam compression, RF, and x-y plane interchange. The dispersion is created by the blue dipoles which have significant edge focusing to complement the red quadrupoles and yellow solenoids to achieve the required tight focusing at the black wedge absorbers. Sextupoles and octupoles in the high dispersion regions will correct chromatic and spherical aberrations. The lower graph is a plan view of the "snake" channel.

PIC POTENTIAL

The PIC effect is related to the absorber material and thickness by

$$\varepsilon \Rightarrow \approx \frac{\sqrt{3}}{4\beta}(Z+1)\frac{m_e}{m_\mu}w;$$

$$wE'_{\mathrm{int}\,r} =< E' > \pi f$$

Where $E'_{\mathrm{int}\,r}$ is the intrinsic energy loss rate of the absorber. Beryllium wedges are favorable since they have low Z, have sufficient density to allow a small *w*, and are technically appropriate in that they can be easily shaped into wedges and refrigerated.

CONCLUSIONS AND OUTLOOK

The transverse emittances of muon beams can be reduced to those normally associated with conventional electron or hadron colliders by implementing Phase Ionization Cooling. This has extremely important consequences for any muon collider design, primarily in the number of muons required for high luminosity.

Some concepts of beam focusing and tune spread compensation for the best parametric resonance cooling and reverse emittance exchange have been proposed. The compatibility of beam resonance focusing with effective exchange is understood. The analytic expressions shown here in the preliminary OptiM design will be used for guidance of simulations.

REFERENCES

[1] Y. Derbenev and R. P. Johnson, *Phys.Rev.STAB* **8**, 041002, (2005).
[2] Y. Derbenev and R. P. Johnson , PAC05, http://snsapp1.sns.ornl.gov/pac05/TPPP014/TPPP014.PDF.
[3] Y. Derbenev and R.P. Johnson, COOL05 http://www.muonsinc.com/reports/COOL05_PIC_and_REMEX_for_MC.pdf.